Modulating mechanism of neuroinflammation following brain ischemic stroke through T cell regulation

Jiwon Kim

The Graduate School
Yonsei University
Department of Medical Science

Modulating mechanism of neuroinflammation following brain ischemic stroke through T cell regulation

A Dissertation Submitted
to the Department of Medical Science
and the Graduate School of Yonsei University
in partial fulfillment of the
requirements for the degree of
Doctor of Philosophy in Medical Science

Jiwon Kim

January 2025

This certifies that the Dissertation of Jiwon Kim is approved

Thesis Supervisor Jong Eun Lee

Thesis Committee Member Young-Min Hyun

Thesis Committee Member Bon-Nyeo Koo

Thesis Committee Member Ho-Keun Kwon

Thesis Committee Member Je Sung You

The Graduate School
Yonsei University

January 2025

ACKNOWLEDGEMENTS

학위과정을 마무리 짓는 이 시점에 어쩔 수 없이 첫 순간이 떠오릅니다. 아주 무더웠던 여름날로 기억합니다. 학부 3학년 여름방학 때 무작정 실험실에 인사를 왔던 그 때는, 연구에 대한 환상을 가지고 제가 대단한 일을 해낼 것으로 착각을 하고 있던 것 같습니다. 하지만 막상 연구를 진행해보니, 그렇지 않다는 것을 깨달았습니다.

아마 그래서일지도 모르겠습니다. 솔직히 말씀드리면 학위를 마무리하고 있는 이 과정 중에도 과학이라는 학문을 통해 우리의 자연과 그 자연에 속한 생명에 대한 진짜 사실을 알 수 있는지에 대해 여전히 의문을 품고 있습니다. 그럼에도 불구하고 끝없는 의심의 심연 속에서도 저와 함께 논의하고 고민해 주신 주변 분들 덕분에 단 하나의 작은 단서라도 제공할 수 있는 사람이 되기 위해 연구를 더 열심히 해야겠다는 마음을 품고 이 작업을 마칠 수 있어서 기쁘게 생각합니다.

이 모든 생각의 중심에 있던 분들에게 감사의 인사를 전하고 싶습니다.

우선 저의 지도 교수님 이신 이종은 교수님,
학부 졸업도 한 참 남아있었던 어리숙한 학생에게 선뜻 실험실에서 인턴을 해보라고 기회를 주신 따뜻함 덕분에 그 인연이 이어져 지금의 제가 있는 줄 압니다. 지도교수로서 그리고 또 어른으로서 언제나 제 편에서 저를 믿어 주시고 단단히 지지해 주셔서 감사드립니다. 연구의 흐름과 의미를 잡아주시고 마지막까지 지도해주신 덕분에 제가 무엇을 놓치고 있는지 부족한 부분에 대해서 많은 내용을 채워 나갈 수 있었습니다. 미숙한 면이 많았지만 정확한 가르침 속에서도 일부는 눈 감아 주시고 보호해 주신 것들 다 기억하고 있습니다. 앞으로 그 마음들을 잊지 않으며 더 성장하도록 노력하겠습니다. 그리고 교수님의 마지막 제자로 남을 수 있어서 개인적으로 너무 의미 있고 뜻깊었습니다. 정말 감사드립니다.

그리고 연구계획서 발표부터 다섯번에 걸친 잦은 심사 일정에도 불구하고 바쁜 시간을 쪼개어 저의 부족한 연구를 성심껏 심사해주신 자문심사 교수님들께 감사 인사를 전합니다.

심사위원장이신 현영민 교수님, 언제나 꼼꼼하게 제가 알아차리지 못하는 부분을 짚어 주시고 실험적 배움이 필요할 때 마다 교수님 랩실 선생님들을 연결해 주셔서 많은 것을 배울 수 있게 되었습니다. 냉정함 속에 따뜻한 마음을 주셔서 그동안 정말 많은 도움을 받았습니다. 감사합니다.

제가 우연한 호기심으로 면역 관련 연구를 하게 되어 심각한 혼란 속에 있을 때 많은 도움을 주신 권호근 교수님, 중간 연구 보고가 끝난 뒤 교수님을 찾아 뵙고 조언을 구했을 때 잘못된 점을 알려주시고 교수님 실험실에서 실험을 직접 보고 배울 수 있게 해 주셔서 면역관련 실험 셋팅에 대해 많은 것을 알게 되었습니다. 진심으로 감사드립니다.

바쁜 수술 스케줄에도 심사에 적극적으로 참여해주시고 연구의 미숙한 연결부분을 지적해주신 구본녀 교수님과 강남 세브란스 응급실에 계셔서 늘 바쁘신 중에 비대면으로 심사에 성심껏 참여해주시고 이메일로 자료를 주고받았던 유제성 교수님께도 깊은 감사의 인사를 드립니다.

그리고 함께 지냈던 실험실 가족들이 생각납니다. 이제는 교수님이 되신 저의 소중한 학부 선배이자 실험실 선배이신 종열 박사님, 박사님 덕분에 제가 이방인이라고 느낀 적 없이 자연스럽게 실험실에 스며들어 적응을 잘 해 나갔습니다. 그리고 연구 스토리를 구성하는 통찰력에 대해서 옆에서 많이 배웠습니다. 나이차가 무색하게 정말 친한 친구처럼 대해 주셨기에 주저 없이 질문하고 자문을 구할

수 있었습니다. 연구에 앞서 함께 연구하는 사람을 어떻게 대하는지가 얼마나 중요한 일인지 박사님을 통해 알게 되었습니다. 정말 감사합니다.

제가 '재미' 라고 부르는 저의 선배 아영 언니, 실험에 대한 토론 요청에 항상 같이 고민해주고 해결책과 노하우를 알려주셔서 현실적인 도움을 정말 많이 받았습니다. 옆 자리에서 동고동락하며 이 생활을 함께 이겨냈다고 생각합니다. 감사합니다.

연구실에서 함께 일하며 크고 작은 도움을 주신 김재영 박사님, 슈미트 박사님, 박주현 박사님, 유새봄 선생님, 지영, 르네, 아라, 서우에게도 감사드립니다. 여러분이 주신 모든 도움을 기억하고 있습니다. 감사합니다.

이 지구상에서 온전히 제 편에 서서 조건 없이 저를 믿어주고 지지해주는 사람은 단 두 명이라고 생각합니다. 엄마, 아빠께 감사를 드립니다. 단 한 순간의 재촉 없이 이 모든 과정을 지지해주시고 제 생각에 동참해 주셨기에 다른 생각 없이 학위 과정에만 몰두할 수 있었음을 깨닫습니다. 무슨 방향으로 우리 삶이 흘러가는지 본질에 대해 늘 고민하는 이상적인 부모님의 사고방식 덕분에 과학에 관심을 가지게 된 것이 아닌가 싶습니다. 표현은 거의 안 하지만 평생 잘 하겠다는 마음을 가지고 있습니다. 감사합니다.

그리고 철학을 공부하는 하나뿐인 동생 지민, 언니가 하는 공부가 자신의 공부와 대척점에 있다고 말하면서도 또 아주 가깝다고 말하는 똑똑한 동생 덕분에 제가 하는 일을 다른 학문의 관점에서도 생각해보고 반성도 많이 했습니다. 동생이지만 언제나 제가 자문을 구할 수 있다는 것이 너무나 든든하고 행복합니다. 감사합니다.

제가 하는 일을 항상 흥미로워하시고 무한한 관심과 응원을 보내주신 할아버지, 할머니, 외할아버지, 외할머니께 감사드립니다. 쉬운 말로 제가 하는 일을 설명 드리는 일이 번거로워서 항상 대충 대답을 드린 것 같아 후회됩니다. 항상 건강하세요, 앞으로 늘 겸손하게 제 자리를 지키는 사람이 되겠습니다. 감사합니다.

그리고 항상 만나면 즐거운 한가람고 16기 친구들 쵸비, 장다, 윤자, 세브언니 묘빈, 혜선이 너무 감사합니다. 사소한 얘기들에 힘을 보태 주고 공감해줘서 많은 의지가 되었습니다.

마지막으로 이 모든 과정의 초석이 되어 주신 존경하는 저의 학부 교수님, 곽한식 교수님께 감사 인사를 드립니다. 2학년 생화학 시간에 지루하게 보였던 각각의 작용들이 왜 일어나고 언제 일어나는지 큰 관점에서 의미를 설명하셨을 때 제가 그 강의실에 앉아있는 이유를 찾았습니다. 그 때 전해주신 교수님의 강의 내용처럼 작은 것을 연구할 때 큰 것을 같이 보면서 하나씩 퍼즐을 맞춰가는 연구자가 되겠습니다. 감사드립니다.

결코 쉽지 않았던 실험실 생활을 마무리하면서, 순수했던 마음보다는 다급한 마음으로 현실에 맞춰 연구를 하지는 않았었나 정말 많은 아쉬움이 듭니다. 하지만 이제 다시 시작인 만큼 예전의 그 생각을 잊지 않고 항상 모든 시작의 기본이 되는 왜? 라는 질문을 품고 사는 연구자가 되도록 노력하겠습니다.

감사합니다.

2025년 1월,
김 지 원 드림

TABLE OF CONTENTS

LIST OF FIGURES

LIST OF TABLES

ABSTRACT

Modulating mechanism of neuroinflammation following brain ischemic stroke through T cell regulation

When an ischemic stroke occurs, it progresses through three major stages: neuroinflammatory response, cell replacement, and functional recovery. Since irreversible neural damage occurs due to the neuroinflammatory response in the initial stage, regulating this first stage is crucial.

In the first stage of the neuroinflammatory response, various cells infiltrate through the disrupted blood-brain barrier. Among them, the cytotoxic T (Cyto T) cells infusing to the infarct site enhance the neuroinflammation. Previous studies have shown that increasing the proportion of regulatory T (Treg) cells relative to Cyto T cells can alleviate inflammatory conditions. Poly-Glu/Tyr polypeptide (Poly-YE; P-YE) has been reported as one of the key immune modulators that regulate T cell balance by recruiting Treg cells and improving behavioral outcomes caused by neurological damage. However, the mechanism is still unclear. Therefore, this study aimed to identify the factors that interact with P-YE and to elucidate how these interactions regulate T cells to alleviate the neuroinflammatory response.

For the protein microarray experiment, P-YE (4.32 mg/mL) was treated on 21,000 protein chips. P-YE loaded on Nanoparticles (Np P-YE; 3ug/mL) was treated to primary Cyto T ($CD8^+$ T) cell isolated from the spleen of 8-week-old C57BL/6 male mouse. These cells were cultured in Oxygen-Glucose Deprivation-conditioned microglia medium (OGD-conditioned medium; CM) to mimic exposure to neuroinflammation. *In vivo* experiment, tMCAO surgery was proceeded and P-YE (1mg/kg) was injected to CCA.

The results showed that P-YE reduced infarct volume following tMCAO surgery and improved the behavioral functions against tMCAO. P-YE strongly bound to neutrophil cytosolic factor (NCF1), which is a part of the NOX complex which secrete ROS in protein microarray experiment. These results identified $CD8^+$ T cells as the target cells for regulation. In the Co-IP experiment, the liberation of Moesin due to the binding of NCF1 to P-YE was confirmed. In the inflammatory response, activated NCF1 is known to bind to Moesin to migrate forward to the membrane and

assemble into the NOX complex.

Additionally, $FOXP3^+$ was expressed in $CD8^+$ T cells in the O+P-YE group. Moreover, in this group, the levels of superoxide and cytokines were remarkably decreased. In tMCAO modeling mice injected with P-YE, $CD8^+FOXP3^+$ T cells were observed around the infarct area. Also, ROS and the pro-inflammatory phenotype of microglia was reduced.

Taken together, NCF1 bound to P-YE can't form NOX complex and Moesin dissociated from NCF1 can lead to FOXP3 expression. Therefore, P-YE binds to NCF1 under neuroinflammatory conditions, converting some $CD8^+$ T cells into $CD8^+FOXP3^+$ cells, thereby inhibiting ROS production and exerting anti-inflammatory effects.

Key words : ischemic stroke, neuroinflammation, poly-YE, $CD8^+$ T cell, treg cell, NCF1, moesin FOXP3, microglia

1. Introduction

This study focuses on reducing damage by regulating adaptive immune cells, specifically T cells, in the neuroinflammatory response following brain ischemic injury. The background of why this research was initiated is as follows:

When an ischemic stroke occurs due to a blood clot in the brain that blocks the supply of oxygen and nutrients, leading to irreversible brain tissue damage, it typically progresses through three major stages[1]. In Phase 1, acute neuroinflammation and cell death accelerate and persist from immediately after reperfusion up to one week. Phase 2 involves the beginning of partial recovery and replacement of damaged tissue, occurring between one week and about one-month post-injury. Finally, in Phase 3, overall tissue remodeling and functional recovery take place. The wider the extent of tissue damage and the higher the number of dead cells from Phase 1, the more challenging the processes in this phase become. Among these three stages, controlling the first stage, where neuronal cell death is accelerated, is the most crucial in minimizing tissue damage. Because preventing tissue damage from the outset is more advantageous for protecting brain function than trying to repair the damaged tissue later. During this stage, various subtypes of immune cells infiltrate the infarcted area through the disrupted blood-brain barrier (BBB), initiating a cascade of inflammatory responses and leading to cellular damage. The types of infiltrating cells vary over time and can interact with resident brain macrophages, such as microglia, influencing both tissue damage and recovery[2].

Myeloid-derived cells, including neutrophils, eosinophils, and basophils, as well as lymphocytes, including T cells and B cells, begin infiltrating and accelerating neuroinflammation from an hour to 3-5 days after reperfusion[3]. Specifically, myeloid cell is among the first to infiltrate and release pro-inflammatory cytokines and reactive oxygen species, exacerbating tissue damage and cell death[4]. However, these cells also participate in clearing debris and facilitating the initial stages of tissue repair, making their role complex and double-edged[5,6].
Also, certain T cells also infiltrate the ischemic brain region alongside myeloid-derived cells during the early stages, triggering a cascade of inflammatory responses[7]. Cytotoxic T cells ($CD8^+$ T cells) begin first infiltrating from hours to day 3 post-reperfusion. In contrast, helper T cells ($CD4^+$ T cells)

exhibit significant infiltration between 24 hours and day 7 post-reperfusion[8]. $CD8^+$ T cells, stimulated by ischemic damage signals, release reactive oxygen species (ROS) and pro-inflammatory cytokines, and induce direct cytotoxic effects by creating pores in neurons, thereby exacerbating tissue damage during acute ischemic stroke[9,10].

$CD4^+$ T cells have various roles depending on their subtype. Th1 and Th17 types primarily function by releasing cytokines like IFN-γ and IL-17, which promote the recruitment of additional immune cells to the site of injury. Another subtype of $CD4^+$ T cells, known as Treg cells, helps in tissue recovery by secreting anti-inflammatory cytokines such as IL-10 [8,11,12]. However, Tregs begin to infiltrate the damaged area only from around day 7 to day 14- after severe damage has already occurred, and their numbers are relatively low. This is because they prioritize adhering to the disrupted BBB to prevent additional immune cell infiltration. Among the infiltrating cells involved in regulating acute neuroinflammation, this research focused on T cells because they play a more sophisticated role in immune responses than myeloid cells and can directly contribute to neuronal regeneration.

Additionally, T cells have distinct subtypes that perform various roles, allowing for targeted modulation of specific T cell types to switch to an anti-inflammatory phenotype or increase the number of cells with this phenotype[13,14]. Therefore, this approach has a higher potential for achieving effective results with minimal side effects compared to targeting innate immune cells, which have limited subtypes.

Among the various types of T cells, $CD8^+$ T cells, in particular, secrete cytotoxic factors to neurons in the early stages and directly induce cell death[15]. Therefore, regulating these types of cells could potentially enhance neuronal survival. However, research on this is highly limited.

While searching for methods to minimize tissue damage by targeting some of the cells that infiltrate early, previous research on a substance called Poly-Glu/Tyr (P-YE) was found[16,17]. These studies demonstrated the effects of P-YE injection following inflammation induced by organophosphate-induced brain injury and middle cerebral artery occlusion (MCAO). The observed effect was that the tissue damage was attenuated due to the increased number of Treg cells at the site of injury, operating their anti-inflammatory function. However, these studies did not provide a detailed explanation of the molecular mechanisms by which P-YE increases the number of Treg cells mediating the anti-inflammatory response, specifically whether other subtypes of T cells are

converted into Treg cells or whether Treg cells migrate from other locations.

Therefore, this study aimed to regulate T cells through P-YE in order to attenuate brain inflammatory responses following ischemic injury. To differentiate from previous studies, it was specifically aimed to identify the specific protein to which P-YE binds during brain inflammatory responses and to elucidate the principles by which this interaction induces cell signaling pathways that convert T cell subtypes into neuroprotective T cells or further promote the migration of existing anti-inflammatory T cells.

To achieve this, a protein microarray was initially performed to identify proteins that bind to P-YE. The cell signaling pathways induced by these bindings, as indicated in the array results, were then investigated, hypotheses were established, and the corresponding data were analyzed. The mechanisms that need confirmation based on the array results are described at the beginning of each results section following the Protein microarray findings (Result 2).

2. Materials and Methods

2.1. Animal

8-week-old C57BL/6 mice were used for all *in vivo* and *ex vivo* experiments and purchased from Orient Bio Science (Gyeonggi, Korea). All mice were taken care in the Specific Pathogen Free zone (SPF zone) of the Avison Biomedical Research Center, Yonsei University College of Medicine during a one-week acclimation period. All experiments involving mice were performed following the ethical guidelines required by the Institutional Animal Care and Use Committee of Yonsei University Health System (IACUC No: 2023-0261) and the National Institutes of Health (NIH).

2.2. Primary cell isolation ($CD8^+$ T cell, Microglia)

2.2.1 Mouse $CD8^+$ T cell isoaltion

To isolate $CD8^+$ T cells, the spleen was isolated from the mouse and the tissue was dissociated using the spleen dissociation kit, mouse (cat.no: 130-095-926, Miltenyi Biotech, Bergisch Gladbach, Germany) with the gentleMACS dissociator (Miltenyi Biotech). The dissociated tissue was processed using the $CD8a^+$ T cell isolation kit, mouse (cat.no: 130-104-075, Miltenyi Biotech), and $CD8^+$ T cells among the various cells in the suspension from spleen were selectively isolated using the autoMACS Pro Separator (Miltenyi Biotech).

2.2.2 Mouse microglia isolation

To isolate microglia, the brain was isolated from the mouse and sliced with 6 pieces.
Sliced tissue was dissociated using the adult brain dissociation kit, mouse and rat (cat. no: 130-107-677, Miltenyi Biotech) with the gentleMACS dissociator. Cell suspesion from the tissue was processed using the CD11b microglia Microbeads, human and mouse (cat.no: 130-093-634, Miltenyi Biotech). Microglia was selectively isolated using the autoMACS Pro Seperator.

2.3. Cell culture and drug treatment

Isolated $CD8^+$ T cells were directly mixed with Dynabeads™ Mouse T-Activator CD3/CD28 (gibco, Waltham, MA, USA) at a ratio of 1:1 for activation and $1x10^6$ cells per well were cultured

in a 24-well cell culture dish with RPMI-1640 medium (Cytiva, Washington D.C., USA) containing 10mM HEPES (Welgene, Gyeongbuk, Korea), 10% FBS (Cytiva), 1% Penicillin-Streptomycin (Cytiva), and 30U/mL rIL-2 (Sigma, St. Louis, MO, USA). In the case of P-YE treatment groups (P-YE and O+P-YE groups), on the day of cell isolation, P-YE (3 μg/mL, Sigma, packaged with PLGA nanoparticles by Comp. Nanoglia, Seoul, Korea) was pre-treated with the $CD8^+$ T cells for at least 6 hours for fusion. OGD-CM treatment groups which contain OGD-CM and O+P-YE groups were treated with a mixture of 70% microglia-derived OGD-CM and 30% RPMI 1640 medium (this proportion was decided according to result of cell viability test '2.6') for 24 hours following the P-YE pre-treatment period. The OGD-CM group that was not treated with P-YE was cultured in regular RPMI medium during the P-YE pre-treatment period, and then this process was carried out. After reacting with OGD-CM, the media was exchanged to RPMI-1640 media to mimic the recovery time after ischemic stroke for 3 days. The media were then directly collected and filtered using a Minisart syringe with a 0.2 μm pore filter (Sartorius, Göttingen, Germany), and the remaining cells were used for other experiments.

Isolated microglia were cultured in RPMI-1640 medium with 10% FBS and 1% P-S. Both types of isolated cells were incubated in an incubator at 37℃ with 5% CO_2.

2.4. Protein microarray

P-YE+FITC (4.32 mg/mL, customized by Bioacts, Incheon, Korea) was used for protein microarray analysis. This analysis was conducted at Geneon Biotech (Daejeon, Korea). In summary, the HuProt™ v4.0 Microarray chip was blocked with 2% BSA solution for 2hrs at room temperature in a shaker. 3 ug of P-YE+FITC (4.32 mg/mL) was added to a microarray chip and incubated with gentle shaking for 8hrs at 4℃. Chip was washed by PBST 3 times and remained fluid was removed completely using a paper towel. The protein microarray was immediately scanned with a GenePix4100A microarray laser scanner (Molecular Devices, Sunnyvale, CA, USA).

2.5. Oxygen-Glucose-Deprivation

To prepare OGD-CM mimicking the ischemic stroke environment for stimulating T cells, after removing the RPMI-1640 medium, microglia were incubated with $BSS_{0.0}$ (Balanced Salt Solution) medium in an anaerobic chamber (37°C, 85% nitrogen, 10% carbon dioxide, and 5% hydrogen) for 50 minutes. After 50 minutes, 5.5 mM glucose was added to the media to mimic reperfusion after

ischemic stroke for 3 days. The media were then directly collected and filtered using a Minisart syringe 0.2 μm pore filter (Sartorius).

2.6. Proteome profiler cytokine array

To identify which cytokines were contained in the collected conditioned media (CM), each sample was analyzed using the Proteome Profiler Mouse Cytokine Array Kit, Panel A (R&D Systems Biotech, Minneapolis, MN, USA), which contains spots with 40 different cytokine antibodies. In summary, a cocktail of 40 cytokine antibodies was mixed with 1 mL of CM for 1 hour at room temperature (RT). This mixture was then applied to the spot panel membrane after blocking for 18 hours at 4℃. After washing, streptavidin-HRP was added to the membrane and incubated on a shaker for 30 minutes at RT. For detection, the Chemi reagent mix was spread on the membrane and visualized using the LAS 4000 mini (Fujifilm, Tokyo, Japan). Intensity and size of each spot was analyzed using OptimEyes Developer (San Francisco, CA, USA), formerly known as HLI image++.

2.7. Cell viability test

Cell death level analysis was performed after the drug treatment. To check the cell death level according to the proportion of OGD-CM, it was mixed with 70%, 50%, and 30% RPMI medium (Cytiva) respectively and treated to the cells for 24hrs. Separately, P-YE (3 μg/mL) was also tested. $1x10^6$ $CD8^+$ T cells in a PDL-coated 35.00 x 10.00 mm confocal dish were washed once and stained with Propidium Iodide (1μg/mL, Sigma) for 10 mins at RT. Each sample was imaged using confocal microscope, LSM 710 (Zeiss, Oberkochen, Germany) equipped with a 20x lens and analyzed using Image J program (NIH, Bethesda, MD, USA).

2.8. Cellular ROS assay

Cellular ROS levels in $CD8^+$ T cells were detected using the DCFDA / H2DCFDA - Cellular ROS Assay Kit (Abcam, Cambridge, UK), and measurement of ROS levels was performed 24 hours after the reaction with OGD-CM. Prepared $CD8^+$ T cells in a PDL-coated 35.00 x 10.00 mm confocal dish were washed once, and 20 μM DCFDA was added to the cells and incubated for 45 minutes at 37°C in the dark. After washing twice, stained cells were imaged using confocal microscopy, LSM170 (Zeiss).

2.9. Western Blot

2.9.1 Whole protein

$1x10^6$ $CD8^+$ T cells or CD11b microglia in 24-well cell culture slide (SPL) were washed by 1xPBS (Biosesang, Gyeongki, Korea) on ice and reacted with 150uL of M-PER™ Mammalian Protein Extraction Reagent (Thermo) mixed with 1x protease inhibitor cocktail (GenDEPOT, Katy, TX, USA) and 1x phosphatase inhibitor cocktail (GenDEPOT) for 30 mins on shaker at 4℃. After 30 minutes, each sample was centrifuged at 14,000g for 10 minutes at 4°C. Each hemisphere, including the infarct area and the contralateral side, was dissociated using a homogenizer in 500 μL of M-PER™ Mammalian Protein Extraction Reagent (Thermo) mixed with 1x protease inhibitor cocktail (GenDEPOT). After 10 minutes, each sample was centrifuged at 14,000 g for 10 minutes at 4°C. The supernatant was collected and directly quantified using the BCA assay with the Pierce™ BCA Protein Assay Kit (Thermo). Samples were loaded into each well of Mini-PROTEAN TGX Stain-Free precast gels (BIO-RAD, Hercules, CA, USA) and run at 100V. Polyvinylidene difluoride (PVDF) transfer membrane, 0.45um pore size (Millipore, Burlington, MA, USA) was laid onto the gel and the protein in the gel transferred to the membrane at for 18hrs at 25V. The membrane was blocked with a 3% BSA solution and reacted with 1'Ab for overnight (O/N) at 4℃.

The following is the list of antibodies used for protein capture. Rat Anti-NOX1 antibody (Dilution Factor: 1:000, Cat.no: ab131088, abcam), Rabbit Anti-CD8 alpha antibody (Dilution F: 1:1000, Cat.no: ab217344, Abcam), Rat Anti-FOXP3 Monoclonal Antibody (Dilution F: 1:500, Cat.no: 14-5773-82, Invitrogen), Rabbit Anti-Moesin (phospho T558, Phospho-specific) antibody (Dilution F: 1:1000, Cat.no: ab177943, Abcam), Rabbit Anti-Moesin (pan-specific) antibody (Dilution F: 1:5000, Cat.no: ab52490, Abcam), Goat NCF1 Antibody (Dilution F: 1:1000, Cat.no: NB100-790, Novus Biologicals, Centennial, CO, USA), Rat mono anti-CD86 (Dilution F: 1:1000, Cat no: ab119857, Abcam), Rabbit anti-CD206 (Dilution F: 1:1000, Cat. No: ab64693, Abcam). After reacting with the primary antibody and washing three times, the membrane was treated with secondary antibodies for 2 hrs at RT. The secondary antibodies used for detecting each primary antibody host are listed below. Goat anti-Rabbit IgG(H+L)-Peroxidase conjugated HRP (Dilution F: 1:5000, Cat.no: sa245916, Thermo). Rabbit anti-Goat IgG(H+L)-HRP conjugated (Dilution F: 1:5000, Cat.no: A27014, Thermo). Goat anti-Rat IgG (H&L) HRP (Dilution F: 1:5000, Cat.no: ab205720, Thermo).

2.9.2 Co-IP

For dectecting protein-protein interaction (NCF1-Moesin binding), Co-IP was proceed following Pierce™ Co-Immunoprecipitation Kit (Thermo). In summary, Goat NCF1 Antibody (Cat.no: NB100-790, Novus Biologicals) was added to 50 µg of each whole protein extraction sample and incubated for 4 hours at 4°C on a rotary mixer. Then, to bind the beads to the NCF1 antibody, 25 µL of washed Protein A/G Sepharose was added to each sample and incubated for 1 hour at 4°C. Each sample bound with Sepharose beads was then collected by low-speed centrifugation (2000g) for 2 minutes at 4°C, and the supernatant was aspirated. After washing the beads three times, 40 µL of 2x SDS-PAGE loading buffer (Biosesang) was added to the samples, and they were boiled for 5 minutes at 100°C to elute the complexes for immunoblotting. The next steps followed the Western blot method. NCF1 was detected in the immunoblotting step using Rabbit Anti-Moesin (pan-specific) antibody (Dilution F: 1:5000, Cat.no: ab52490, Abcam) and Goat anti-Rabbit IgG(H+L)-Peroxidase conjugated HRP (Dilution F: 1:5000, Cat.no: sa245916, Thermo).

In both whole protein and Co-IP experiments, West-Q Pico Dura ECL solutions A and B (GenDEPOT) were mixed in a 1:1 ratio and applied to the membrane for 20 seconds at room temperature. The membrane was visualized using the LAS 4000 mini (Fujifilm), and the detected images were analyzed using the Image J program (NIH).

2.10. Immunocytochemistry

$1x10^6$ cells in 0.01% Poly-L-Lysine (Sigma) coated 4-well cell culture slide (SPL) were washed with 1x PBS at once. 3.7% Paraformaldehyde (PFA; Sigma) was used for cell fixation for 15mins at ice. Cells were permeabilized with 0.1% triton X-100 (Sigma) for 8 mins at ice (Each step included 3 times washes.) and blocked with 3% BSA solution for an hour at ice. 1'Ab: Rabbit Anti-CD8 alpha antibody [EPR21769] (Dilution F: 1:500, Cat.no: ab217344, Abcam), Rabbit Anti-CD11b antibody [EPR1344] (Dilution F: 1:1000, Cat no: ab133357, Abcam) and Rat Anti-FOXP3 Monoclonal Antibody [FJK-16s] (Dilution F: 1:500, Cat.no: 14-5773-82, Invitrogen) were treated to samples and incubated for o/n at 4°C and after washing 3 times, 2'Ab: Donkey anti-Rabbit IgG (H+L)-FITC (Dilution F: 1:1000, Cat no: ab6798, Abcam), Goat Anti-Rabbit IgG (H+L)-Rhodamine (Dilution F: 1:1000, Cat no: 31686, Invitrogen), Goat anti-Rabbit IgG (H+L) Alexa Fluor™ Plus 555 (Dilution F: 1:1000, Cat no: A32732, Invitrogen) and Goat anti-Rat IgG (H+L)

Rhodamine (Dilution F 1:1000, Cat no: 31680, Invitrogen) were incubated for 2hrs at RT. To stain nucleus, 1x DAPI (Thermo) was treated for 5 mins at RT. ProLong Glass antifade mountant (Invitrogen) was dropped onto the 24 x 50 mm cover glass (Marienfeld, Lauda-Königshofen, Germany) and this was placed over the slides. Each sample was imaged using confocal microscopy (LSM 710, Zeiss), and the data was analyzed using the ZEN blue program (Zeiss).

2.11. Flow cytometry

$1x10^6$ $CD8^+$ T cells were prepared in each sample, the CD3/CD28 beads bound to T cells were removed with DynaMag™-2 (Invitrogen), and the cells were washed once with 1x PBS. First of all, surface target was stained with PE^{Cy7} Rat anti-mouse CD8a (1:100, Cat.no: 552877, Becton, Dickinson and Company; BD, Franklin Lakes, NJ, USA) for 30 mins at 4℃. After then, samples were washed 3 times and centrifuged 400g for 5mins at 4℃. Secondly, each sample was fixed and permeabilized following Foxp3 / Transcription Factor Staining Buffer Set (eBioscience™, San Diego, CA, USA). After diluting the Fixation and Permeabilization Concentrate with Diluent at a 1:3 ratio, the mixture was added to each sample and incubated at RT for 1 hr (100 µL per microcentrifuge tube). After washing 3 times (centrifuged at 400g for 5 minutes at RT) with 1x permeabilization buffer, nuclear protein was finally stained with PE Rat anti-mouse FOXP3 (1:100, Cat. no: 563101, BD) for 30 minutes at RT and washed 2 times with 1x permeabilization buffer and 1 time with PBS. After washing, 300 µL of FACS staining (Invitrogen) buffer was added to the samples. To establish standard for significant fluorescence expression regions, negative and positive controls were separately prepared. Negative con was prepared using Anti-Mouse Ig, κ / Negative control compensation particle set (60uL, Cat.no: 552843, BD) and Positive con was prepared using compensation beads (60uL) with PE-Cy7 Mouse IgG1k Isotype control (1:100, Cat.no: 565573, BD), PE Mouse IgG1, κ Isotype Control (1:100, Cat.no: 550617, BD), FITC Mouse IgG2b, κ Isotype Control (1:100, Cat.no: 555057, BD) for 30mins at RT. Each sample was moved onto 5mL Polystyrene Round-Bottom Tube with Cell Strainer Cap (Falcon, Corning, NY, USA) and read with FACSymphony A5 (BD). Each of the data sets was thoroughly reanalyzed later using the FlowJoTM v10 software (BD).

2.12. tMCAO surgery

Mice were anesthetized with Zoletil (30mg/kg, Virac, France) mixed with Rompun (10mg/kg, Bayer, Germany) administered as an intraperitoneal (i.p.) injection. The skin was incised from below the jaw to the chest. Carefully dissecting the artery and nerves, the Common Carotid Artery (CCA) and External Carotid Artery (ECA) were permanently tied with 1 cm of 5-0 black silk suture. The bifurcation of the ECA and Internal Carotid Artery (ICA) was temporarily tied off with a ribbon tie. A small hole was made 1mm in front of the permanently ligated CCA to allow the insertion of a suture. The MCAO suture was inserted through the hole, and the temporarily tied ribbon tie was slightly loosened to allow the suture to enter the middle cerebral artery from the ICA. To prevent micro blood leakage, the ribbon tie was tied over the inserted MCAO suture and remained the occlusion for 40 mins. After then, MCAO suture was slowly removed and ICA was permanently tied. Separately, in the P-YE group, P-YE (1.5mg/kg) was injected into the MCA region from the ICA using a 32G catheter 112mm tube (WPI, Sarasota, FL, USA). To reduce tissue adhesion, a drop of saline was applied to the tissue and the incised skin was then carefully sutured to prevent infection and disinfected with povidone.

2.13. In vivo ROS assay

After reperfusion following tMCAO surgery, dihydroethidium (DHE, 1 mg/kg), which binds to ROS, especially O_2^- was injected into the MCA region via the ICA using a 32G catheter 112 mm tube (WPI). For the P-YE group, DHE was directly injected following P-YE administration. oxidized DHE (Ethidium; Eth+) was detected Ex/Em: 510/605nm wavelength using confocal microscopy (LSM 710, Zeiss) and the data was analyzed using the Image J Program (NIH).

2.14. TTC staining

2,3,5-Triphenyltetrazolium Chloride (TTC) stains mitochondrial dehydrogenase. As a result of ischemic damage, if cells die, mitochondrial dehydrogenase is not released, and thus, the tissue does not stain. Three days after tMCAO surgery, the mouse was sacrificed and perfused with 0.9% normal saline only. The brain was isolated and sliced into 2mm sections. The isolated brain was placed in a 2% TTC (Sigma) solution and incubated in 37°C water baths for 30 mins. The size of the infarct area was analyzed using the Image J program (NIH).

2.15. Immunohistochemistry

The mice were sacrificed by cardiac perfusing using 0.9% normal saline and 3.7% PFA and the brain was sectioned as 2mm. Sectioned tissue was refixed with 3.7% PFA for 2 days at 4°C to allow for penetration PFA from the outside and reacted with 30% sucrose including 0.1% sodium azide (Sigma) for 2 days at 4°C. 2mm tissue was embedded in a cryomold with Tissue-Tek® O.C.T. Compound (Sakura, Torrance, CA, USA) and directly frozen in a -80°C deep freezer. Frozen tissue was sliced as 14um and attached to the slide glass. To remove the remaining OCT compound around the tissue, samples were washed once with 1x PBS for 5 mins at RT. Fixation and permeabilization were performed with 3.7% PFA and 0.1% Triton X-100, respectively, for 10 minutes at RT (including 3 washes in each step) and samples were blocked with 5% BSA solution for 1hr at RT. 1'Ab was reacted to samples for o/n at 4°C. 1'Ab list: Rat mono anti-CD86 (Dilution F: 1:200, Cat no: ab119857, Abcam), Rabbit anti-CD206 (Dilution F: 1:200, Cat. No: ab64693, Abcam), Rabbit anti-CD8 alpha antibody (Dilution F: 1:100, Cat.no: ab217344, Abcam) and Rat anti-FOXP3 Monoclonal Antibody (Dilution F: 1:100, Cat.no: 14-5773-82, Invitrogen). After washing, 2'Ab was reacted to samples for 2hrs at RT. 2'Ab list: Goat Anti-Rat IgG H&L Alexa Fluor® 488 (Dilution F: 1:1000, Cat no: ab150157, Abcam), Goat Anti-Rabbit IgG (H+L)-Rhodamine (Dilution F: 1:1000, Cat no: 31686, Invitrogen), Donkey anti-Rabbit IgG(H+L)-FITC (Dilution F: 1:1000, Cat. no: ab6798, Abcam), Goat anti-Rat IgG (H+L) Rhodamine (Dilution F 1:1000, Cat no: 31680, Invitrogen). To stain nucleus, 1.5x DAPI (Thermo) was treated for 5 mins at RT. ProLong Glass antifade mountant (Invitrogen) was dropped onto the 24 x 50 mm cover glass (Marienfeld, Lauda-Königshofen, Germany) and this was placed over the slides. Each sample was imaged using confocal microscopy (LSM 710, Zeiss), and the data was analyzed using the ZEN blue program (Zeiss).

2.16. Behavior test

To test the injury and recovery levels of neurological functions after tMCAO surgery, three type of validated behavior test[18] was conducted.

2.16.1 Grip strength test

A grip strength test, which can evaluate the impact of central nervous system damage on muscle strength and motor function, was conducted. Gently holding the mouse by its tail, the forepaws were placed on the metal grip bar of the grip strength measurement device. The tail was pulled backward

until the mouse released the grip bar and the score recorded on the screen was checked.

2.16.2 Bederson score

To evalutate acute ischemic stroke effect, the bederson score was calculated by observing circling behavior. The objective grading criteria are as follows. Grade 0: It was assigned when the mouse didn't show any other defects. Grade 1: When the mouse shows very mild signs of paralysis, such as trembling its forepaws when lifted. Grade 2: This score is assigned when mild body tremors and a decrease in motor function on the paralyzed side begin to appear. Grade 3: This score is assigned when movement towards the paralyzed direction decreases and as that result, unilateral circling behavior is observed. Grade 4: This score is assigned when periodic circling behavior and intermittent seizure symptoms are observed. Grade 5: The mouse didn't show any movement when touched on its back, including symptoms of grade 4.

2.16.3 Garcia scale

In addition to the Bederson score, the functional outcomes of mice after surgery were evaluated by performing and summing the scores of some parts of several neurological tests developed by Garcia. Spontaneous activity (0–3), Symmetry of limb movement (0–3), Symmetry of response to stimuli (0-3), Direction of rotation when lifted by the tail (0-3) was conducted and the greater the ischemic damage, the worse the activity in the affected area, resulting in lower scores.

2.17. Statistical analysis

The quantification analysis was proceed using Prism software developed by GraphPad (San Diego, CA, USA). When there were only two groups, a T-test was used for analysis, and when there were three or more groups, one-way ANOVA was performed for analysis followed by Bonferroni's post hoc test. A P-value of less than 0.05 was considered statistically significant.
(*P<0.05, **P<0.01, ***P<0.001)

3. Results

3.1. Injection of P-YE after tMCAO surgery reduced the infarct size and lessened the effects of ischemic damage

Before confirming the mechanism, to primarily determine whether P-YE can mitigate ischemic damage *in vivo*, P-YE was injected after performing transient middle cerebral artery occlusion (tMCAO) surgery. The tMCAO surgery was performed following the protocol outlined in '2.12.' (Fig. 1A). The CCA and ECA were permanently tied, while the branching point was transiently tied. The 6-0 MCAO suture was inserted through a small hole in front of the CCA and advanced near the MCA. After 40 minutes of occlusion, P-YE was injected into the CCA simultaneously with reperfusion (Fig.1B). After tMCAO surgery, TTC staining was indicate distinguishing between viable and necrotic cells in brain tissue (Fig.1C). The results showed that in the coronal section, approximately half of the tissue area was necrotic due to infarction in tMCAO group, while the group injected with P-YE (tMCAO+P-YE; tM+P) showed a reduction of about 1.8 times (Fig.1D).

In the grip test, after tMCAO surgery, grip strength decreased by approximately 6 times compared to the sham group, but increased by 4.5 times following P-YE injection (Fig.1F). The Bederson score averaged 3.8 in the tMCAO group and 2.1 after P-YE injection (Fig.1H). The Garcia score was 2.2 folds lower than sham in the tMCAO group and after P-YE injection, the score was 1.4 folds higher (Fig.1I).

Therefore, as demonstrated in previous studies, P-YE also reduced tissue damage and improved behavioral issues caused by cerebral ischemic injury in the actual experiment.

A)

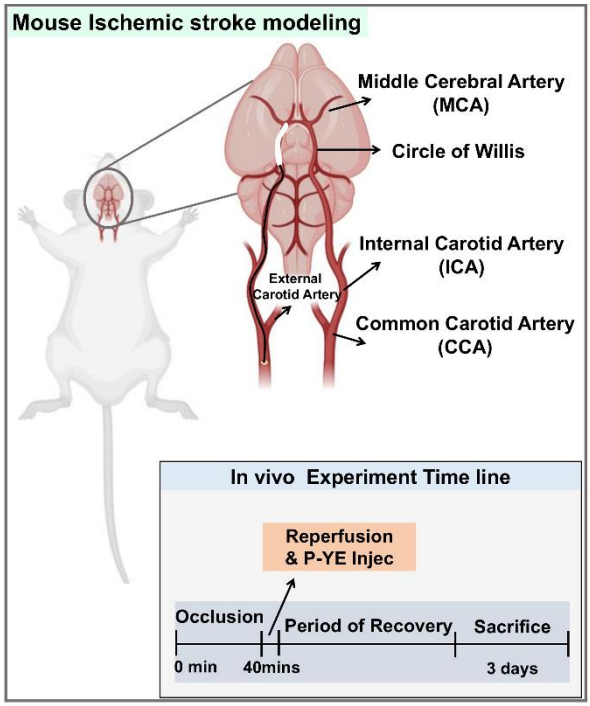

B)

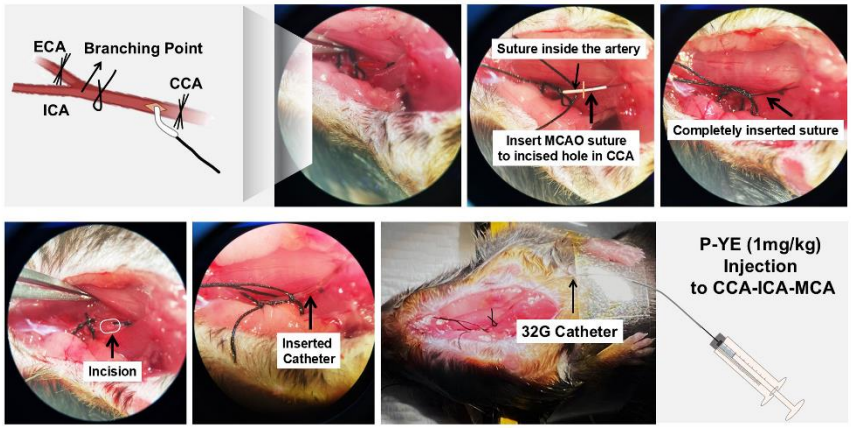

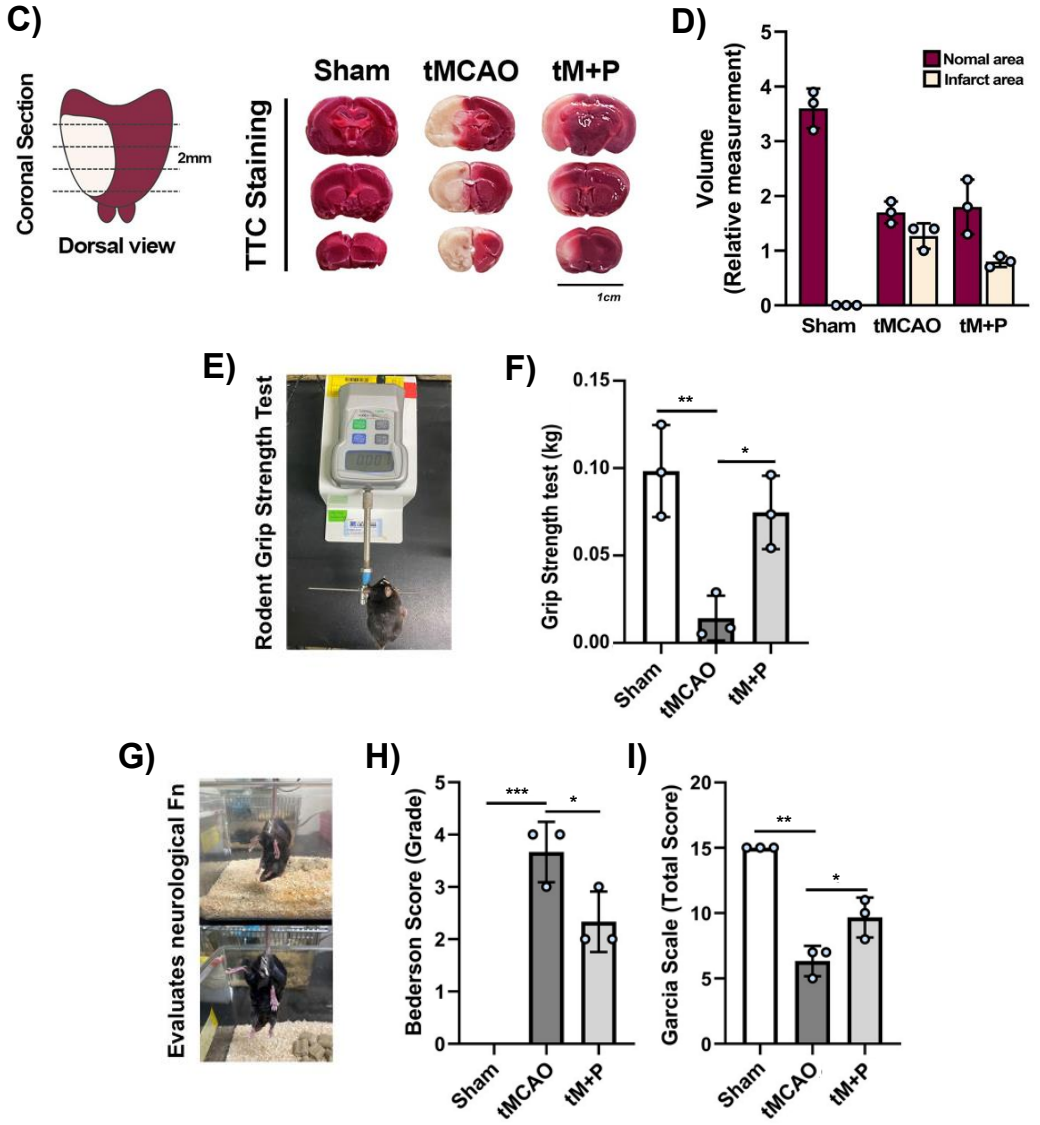

Fig 1. Process of tMCAO surgery and confirmation of the effect observed after P-YE injection following tMCAO surgery. A) Timeline of *in vivo* experiments. B) The location where the blood vessel is tied during tMCAO surgery and photos of the actual surgery process. C and D) The results of TTC staining on coronal sections of tissue after the surgery. E-I) Quantification results of behavioral tests demonstrating the protective effects of P-YE against damage. (***P-value<0.001, **P-value<0.01, *P-value<0.05, n=3)

3.2. P-YE was strongly bound to 5 types of proteins: NCL, BDH2, PRB3, NCF1, and HNRNPAB among 21,000 proteins

To identify which protein binds to P-YE, proteome microarray chip was conducted. The P-YE, which has a co-polymer structure with glutamic acid and tyrosine randomly ligated, was used in the microarray analysis with FITC tagged (Fig.2A). Detected images showed all signals of 21,000 protein spots and the selected top 1% fluorescence signals with noise removed among them (Fig. 2B). Among the top 1% of proteins with the highest A-scores, 8 types of proteins displayed stronger signal intensity scores compared to other bindings, and 5 of these proteins—Nucleolin (NCL), 3-Hydroxybutyrate Dehydrogenase 2 (BDH2), Proline Rich Protein BstNI Subfamily 3 (PRB3), Neutrophil Cytosolic Factor 1 (NCF1), and Heterogeneous Nuclear Ribonucleoprotein A/B (hnRNP A/B)—showed even higher scores, indicating a stronger binding to the sample protein (Fig.2C). In brief, the functions of the five candidate target proteins are as follows: NCL has functions of Ribosome Biogenesis, RNA Stabilization, Cell Proliferation, and Anti-Cancer Effects. BDH2 is an enzyme which converts β-hydroxybutyrate to acetoacetate[19] and related to Iron Homeostasis[20]. PRB3 is found in saliva and it maintain oral health. NCF1 is a one compartment of NADPH Oxidase and promote ROS production in immune response[21]. Hn RNP A/B is related to RNA splicing and transport[22]. Among these Proteins, NCF1 was selected as a target protein interacted with P-YE, because it was the only factor directly involved in the T cell immune response after ischemic stroke (Fig.2D). Based on these results, a more detailed investigation into NCF1 was conducted to develop a hypothesis regarding the actions that could be inhibited or promoted when NCF1 binds with P-YE. NCF1, as a component of the NOX complex, is guided by phosphorylated Moesin to assemble into the NOX complex, leading to the release of ROS[21]. Therefore, in the subsequent results, it was examined whether the binding of NCF1 to P-YE after P-YE treatment could inhibit these existing cytotoxic functions by targeting $CD8^+$ T cells that infiltrate and release ROS early after cerebral ischemic injury.

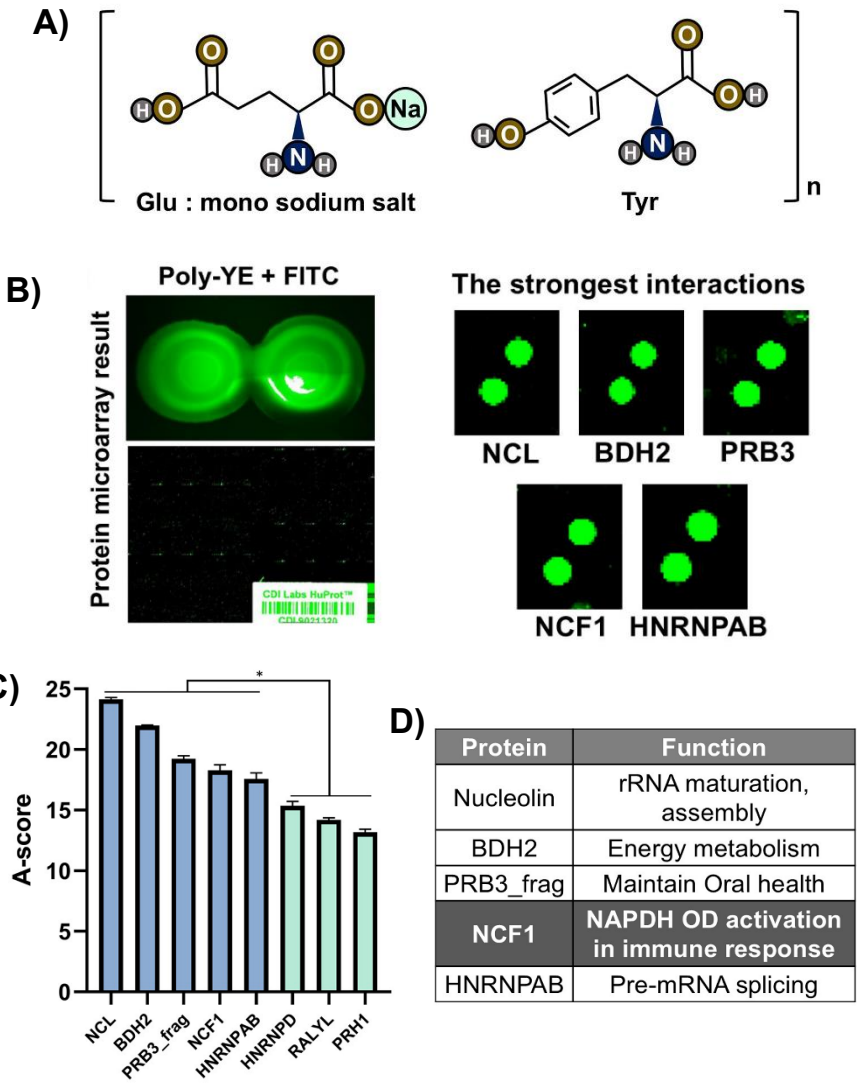

Protein	Function
Nucleolin	rRNA maturation, assembly
BDH2	Energy metabolism
PRB3_frag	Maintain Oral health
NCF1	**NAPDH OD activation in immune response**
HNRNPAB	Pre-mRNA splicing

Fig 2. Chemical structure of P-YE and comfirmation of P-YE+protein binding by protein microarray chip. A) Chemical structure of P-YE (5~15kDa). It is randomly composed of Glutamic acid and Tyrosine. B and C) Scanned microarray chip shows signal intensity of 21,000 human protein. Among that, 5 type of proteins: NCL, BDH2, PRB3, NCF1, HNRNPAB has the highest A-score. D) Among the five candidate proteins, NCF1 was selected as the final target protein to investigate the interactions with P-YE because its function is most closely related to T-cell immunity. (*P-value<0.05, n=3)

3.3. P-YE packaged PLGA-nanoparticle can enter the cytoplasm of T cells

To enhance the cellular permeability of P-YE (5~15 kDa), it was packaged with a Poly-Lactic Acid-Glycolic Acid (PLGA)-based nanoparticle. PLGA consists of lactic acid and glycolic acid, which can enter the cell membrane through pinocytosis, a type of endocytosis, and then undergo the Krebs Cycle to be degraded into CO_2 and H_2O (Fig.3A, B). Before P-YE treatment to the cells, CD8 expression was confirmed by Immunocytochemistry (ICC). It was imaged with 63x oil lense and zoomed 3 folds. CD8 was expressed surface of the cells centered nucleus (Fig.3C). Also, entrance of P-YE tagged with FITC was confirmed by ICC. The presence of P-YE was confirmed in the region between the nucleus and CD8 (Fig.3D). Through this, it was confirmed that P-YE was successfully delivered to the cytoplasm. The number of cells introduced with P-YE was quantitatively assessed through flow cytometry. To accurately gate the area of cells introduced with P-YE+FITC, the FITC positive control was first analyzed, and it was confirmed that detection occurred in the region above 10^3 (Fig.3E). In Con group, over 99% T cells were detected in the region below10^3 and P-YE treatment group, cells of approximately 30~55% was contained P-YE (Fig.3E, F and G). In other words, when treated with P-YE, the proportion of cells fused with P-YE Np was approximately half of the total cell population.

In summary, the uptake rate of P-YE into the cells was approximately 40%, and it was confirmed that the introduced P-YE was successfully delivered to the cytosol.

A) Structural formula of PLGAs- Nanoparticles

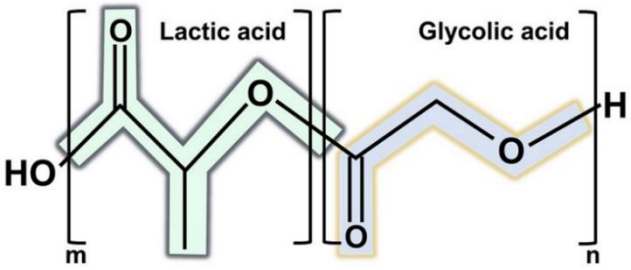

B) Nanoparticles loaded with P-YE

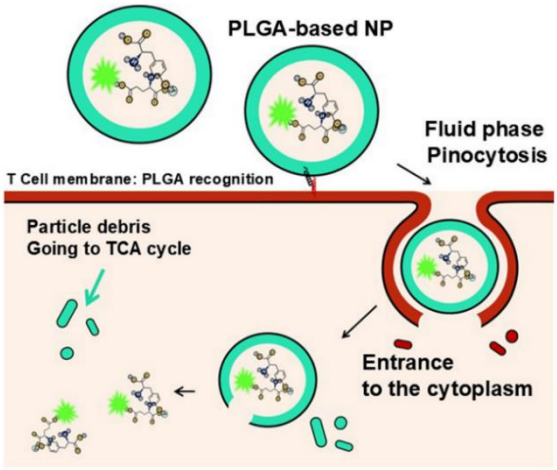

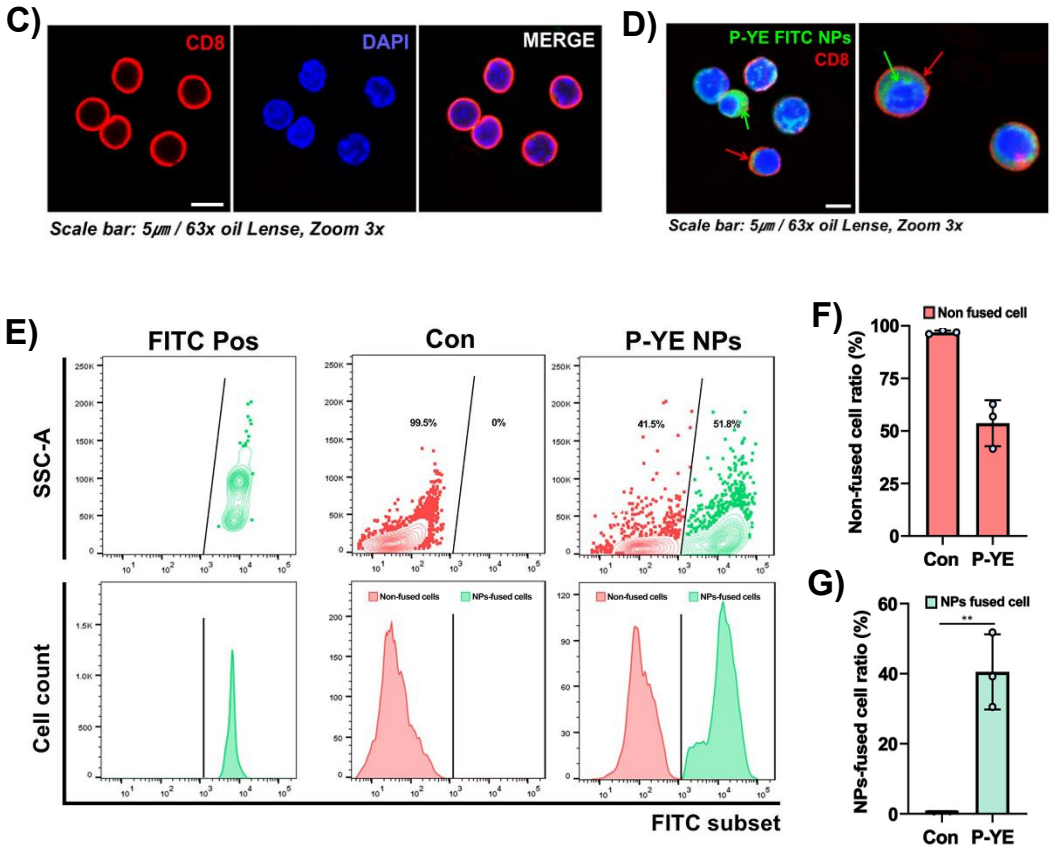

Fig 3. Mechanism of P-YE entry into cells and confirmation of P-YE introduction inside the cells by ICC and Flow cytometry. A) Chemical structure of PLGA Nanoparticle. Np is consisted of Lactic acid and Glycolic acid which can biodegraded by CO_2 and H_2O by Krebs cycle. B) PLGA Nanoparticle fuse to cell membrane by pinocytosis and introduce to cytosol. C, D) ICC data shows that isolated CD8+ T cells expressed CD8 on the surface of the cells, and the introduction of P-YE into the cytosol was confirmed. E, F and G) Flow cytometry results for quantifying the number of cells introduced with P-YE showed that approximately half of the total cells were introduced with P-YE. (**P-value<0.01, n=3)

3.4. Microglia-derived OGD-CM sup for stimulating T cells contained pro-inflammatory cytokines, and it affected $CD8^+$ T cell viability

To mimic the reperfusion environment that stimulates infiltrating $CD8^+$ T cells in ischemic stroke, isolated microglia underwent the OGD process following methods '2.5' (Fig.4A, B). Isolated microglia was confirmed CD11b expression (Fig.4C). Effected OGD environment microglia was secreted over 10 types of cytokines, especially IFN-γ, TNF-α, and SDF-1 (Fig.4 D, E). IFN-γ and TNF-α induces tissue damage response[23], inflammatory response and apoptosis[24]. Additionally, since the cytokine array panel did not include TGF-beta, a key factor that can stimulate T cells, it was separately confirmed through WB whether ischemic microglia were expressing it. TGF-beta was expressed in microglia stimulated by OGD (Fig.4F, G).

These secreted factors can efficiently induce Moesin which guide NCF1 toward to the membrane phosphorylation in $CD8^+$ T cells[25,26]. Before confirming phosphorylation, a cell viability test was primarily conducted to examine the effect of OGD-CM containing these toxic factors on T cell apoptosis. In OGD-CM 100% group, over 80% of the seeded cells underwent apoptosis, and in the 70% OGD group, approximately 30% of the cells showed apoptosis. Cell death was barely detected in the 30% and 50% OGD-CM groups, whereas the 100% supernatant exhibited a cell death rate that was roughly three times higher than that observed in the 70% group (Fig.4H, I). Therefore, the 70% OGD-CM supernatant was selected as the condition for treating $CD8^+$ T cells.

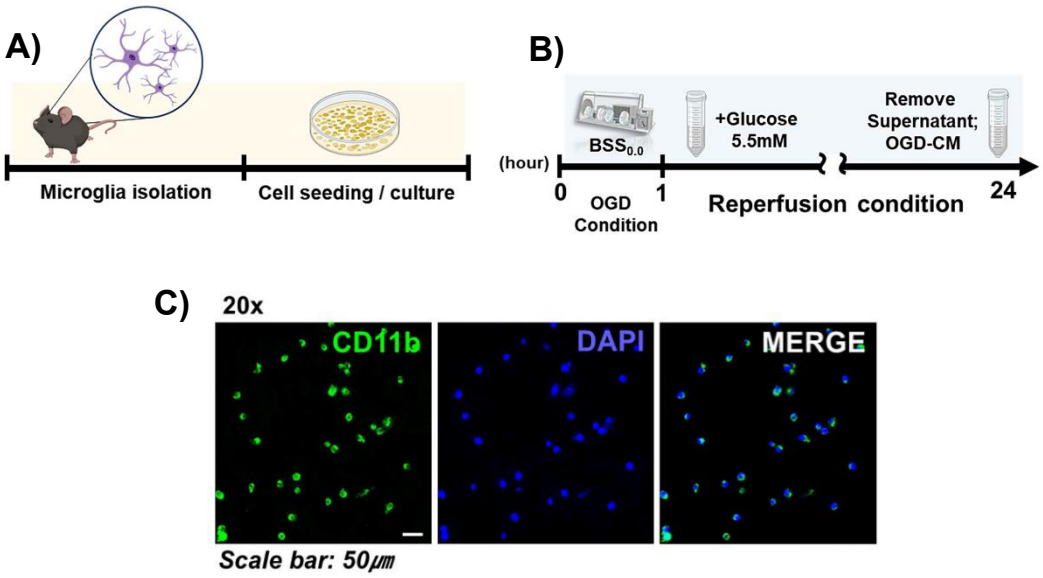

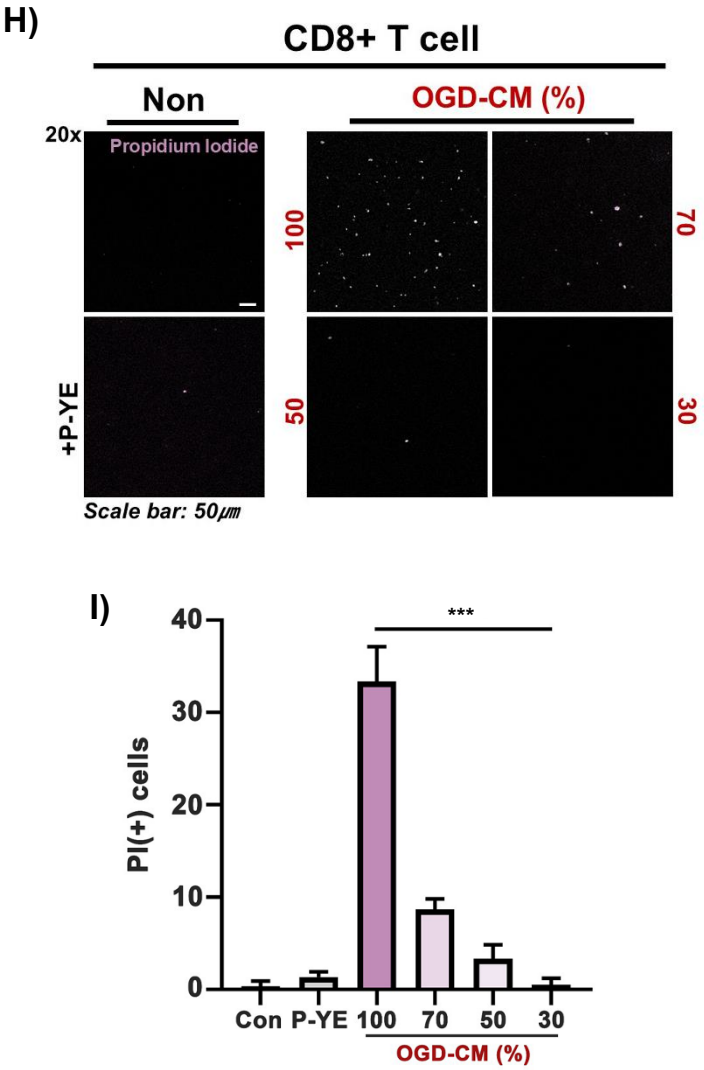

Fig 4. Confirmation of CD11b expression in isolated microglia, cytokine array results from microglia-derived OGD-CM, and CD8$^+$ T cell viability test results due to OGD-CM. A and B) Experimental timeline for obtaining microglia OGD-CM. C) In ICC data, CD11b was expressed in isolated microglia (Scale bar: 50um). D and E) In microglia derived OGD-CM group, IFN-γ, TNF-α and SDF-1 was highly expressed. F and G) OGD-reacted microglia was expressed TGF-β. H and I) Cell viability test results using PI staining (Scale bar: 50um). 100% OGD-CM group is about 3.5 folds higher than 70% group and 7 folds higher than 30% group. (***P-value<0.001, n=3)

3.5. NCF1-Moesin complex was decreased after P-YE treatment

The amount of the NCF1-Moesin complex, which interacts during inflammatory responses[21,27], was confirmed to determine whether it changes when P-YE enters the cells.

In Co-ip data, to determine the amount of Moesin bound per unit of NCF1, the input was quantified and loaded to show the expression of an equal amount of NCF1 (Fig.5C). The quantification data of Co-ip showed that the level of NCF1-Moesin binding complex per unit of NCF1 in OGD-CM group was about 1.75 folds higher than in the O+P-YE group (Fig.5D).

Additionally, since Moesin has an unfolded structure when it is bound to other factors, its C-terminal is basically phosphorylated[28]. Therefore, theoretically, if NCF1 is bound to Moesin, the amount of phosphorylated Moesin should increase proportionally to the amount bound. To verify this, western blot (WB) was peformed on whole protein extracts and proteins were detected with a pan-specific Moesin antibody (Fig.5E). The results showed that the OGD-CM group showed approximately a 1.35-fold higher ratio of phosphorylated Moesin compared to the Con and P-YE groups, while the O+P-YE group showed an approximately 1.8-fold higher (Fig.5F, G). Meanwhile, the overall expression level of NCF1 within the cells did not show significant differences across all groups (Fig.5E, H).

Taken together these results, it is interpreted that the amount of phosphorylated Moesin increased in both the OGD-CM and O+P-YE groups due to the inflammatory stimuli. However, in the O+P-YE group, despite the phosphorylation of Moesin, the decrease in the amount of the NCF1-Moesin complex can be attributed to NCF1 binding with P-YE. Furthermore, NCF1 appears to be consistently expressed under all conditions and functions in cooperation with other factors in specific environments, such as inflammatory conditions, without changes in its expression levels.

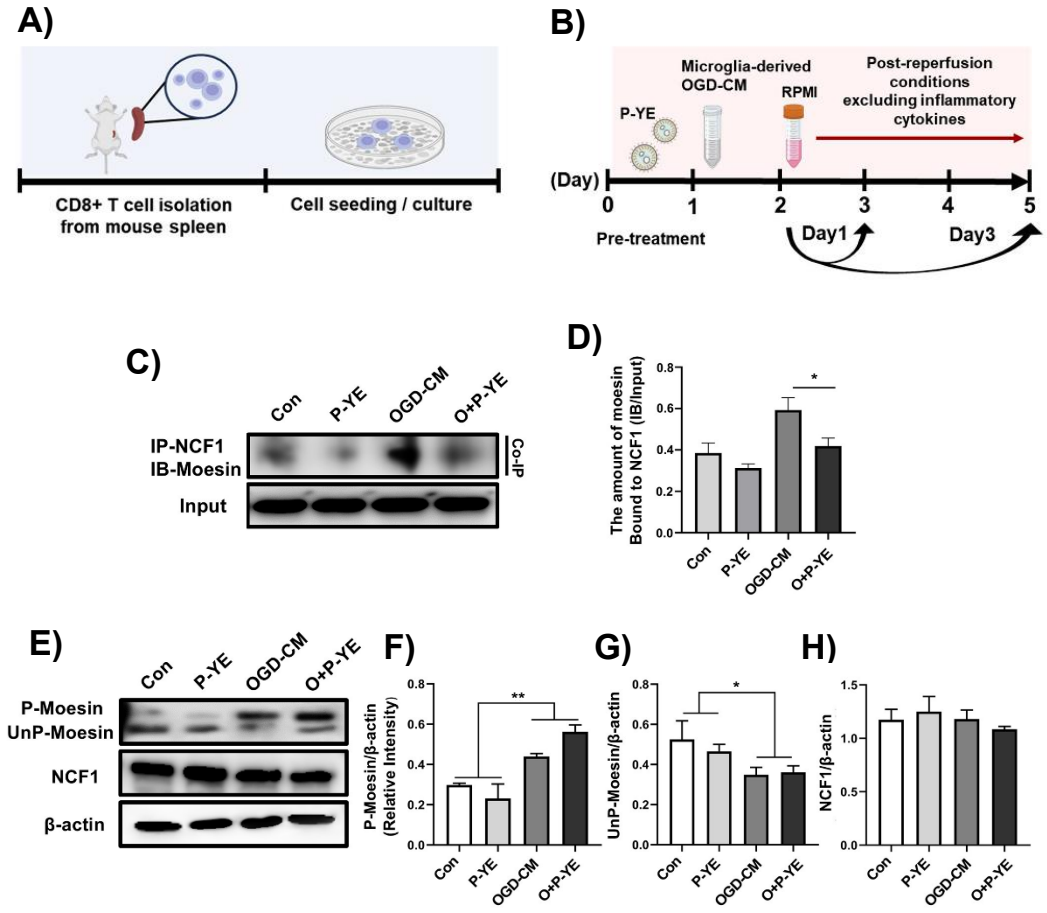

Fig 5. Assessment of molecular-level changes (NCF1 and Moesin) induced by P-YE treatment. A and B) An experimental setup to mimic the environment encountered by T cells during ischemic stroke. C) Co-ip data indicates amount of NCF1-Moesin binding complex. D) The quantification data shows the difference in the amount of complex between groups. (*P-value<0.05, n=3) E) WB data shows the Moesin phosphorylation/unphosphorylation and the difference in NCF1 expression levels in total protein. F, G and H) The quatification data shows amount of the P-Moesin/UnP-Moesin and NCF1 in each group. In summary, P-mosein was higher in OGD-CM and O+P-YE groups but, Un-P Moesin was the opposite. NCF1 was consistently expresssed in all gorups. (**P-value<0.01, *P-value<0.05, n=3)

3.6. FOXP3 was expressed with simultaneous OGD-CM and P-YE treatment

Several studies have shown that Moesin can mediate the expression of FOXP3 under stimulated by TGF-beta conditions. Consequently, this step aimed to determine whether Moesin, in its unbound state following P-YE treatment under inflammatory conditions, could also induce FOXP3 expression[26], potentially inducing anti-inflammatory functions in $CD8^+$ T cells.

To confirm FOXP3 expression, ICC, WB and Flow cytometry were performed. CD8 expression on the cell surface supports that FOXP3 expression was confirmed specifically in $CD8^+$T cells, not in other cells in ICC data. Treated P-YE (FITC signal) was confirmed in cytosol and in that group, FOXP3 was expressed in nucleus area (Fig.6A). However, it is unclear that FOXP3 expression confirmed only ICC. Therefore, WB and flow cytometry were conducted to quantify FOXP3 expression. The WB results showed that in O+P-YE group, FOXP3 was expressed about 5 folds higher that other groups but, it showed a significantly lower expression level compared to the expression level of CD8 (Fig.6B, C and D). Flow cytometry data showed that, in the O+P-YE group, FOXP3 expression was observed in approximately 15% of the total analyzed cells, and FOXP3 was selectively expressed only in the cells where P-YE had been introduced (light green dot). When considering only the cells into which P-YE was introduced, rather than the entire cell population, the expression level of FOXP3 was calculated to be 24%. And in the other groups, FOXP3 expression was observed at levels ranging from 0.5% to 2% (Fig.6E, F, G and H). When integrating the results with 3.4, it is interpreted that P-YE, introduced simultaneously with the inflammatory response, binds with NCF1, allowing the phospho-Moesin, which now exists alone, to enter the FOXP3 expression signaling pathway instead of the previously dominant NCF1-mediated pathway.

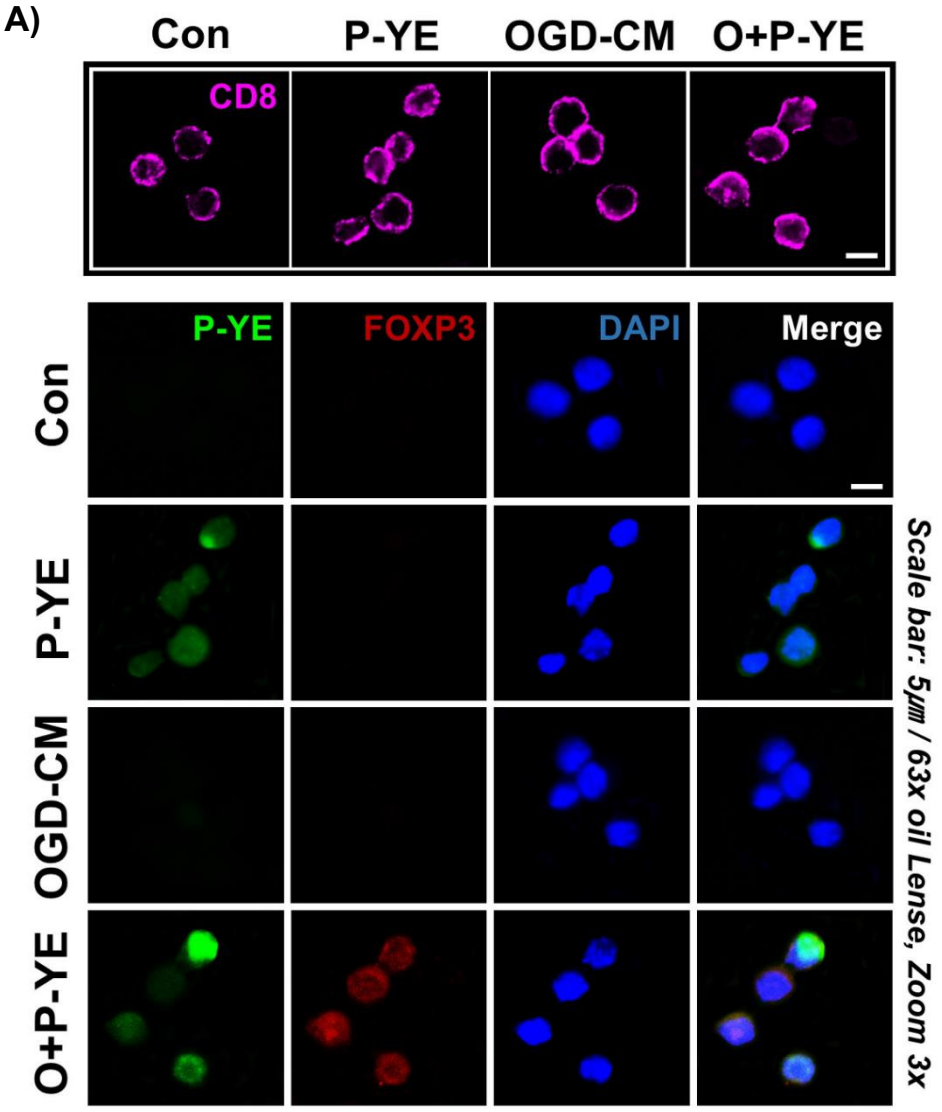

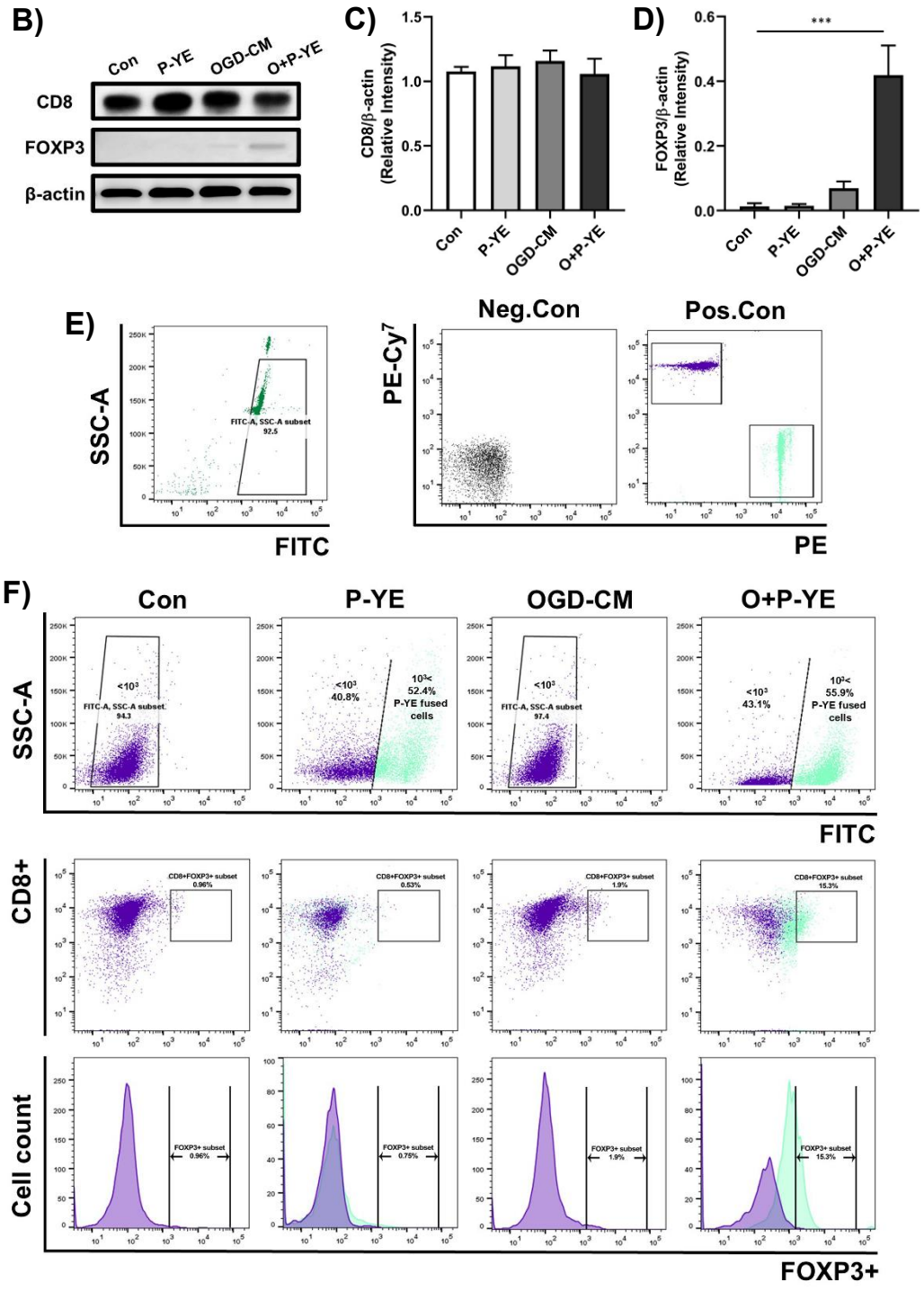

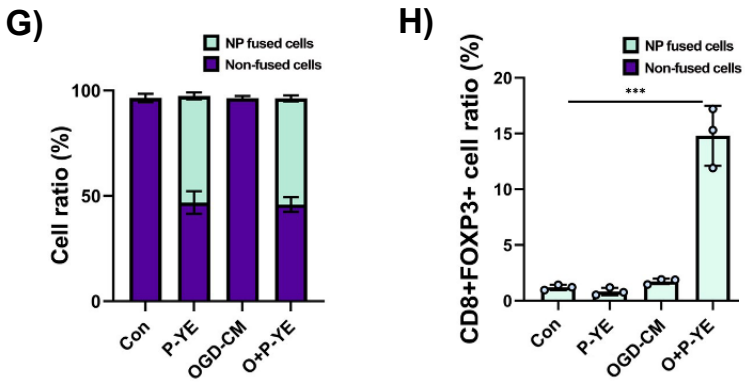

Fig 6. Confirmation of CD8 and FOXP3 expression levels following P-YE treatment. A and B) ICC and WB data show expression of CD8 and FOXP3 (Scale bar: 5um). C and D) The quantification data show the differences of CD8 and FOXP3 expression between the groups numerically. E) Control data for establishing the reference regions of CD8 and FOXP3 expression. F) Flow cytometry data show that the proportion of cells where P-YE has entered among the total $CD8^+$ T cells, along with the expression levels of CD8 and FOXP3 in both P-YE-fused cells and P-YE-non-fused cells. G and H) The quantification data numerically demonstrate the proportion of P-YE entry and the expression levels of CD8 and FOXP3. (***P-value<0.001, n=3)

3.7. In inflammatory conditions, the levels of ROS and the expression of NADPH Oxidase were decreased by P-YE

These results were confirmed whether Reactive Oxygen Species (ROS) release is actually reduced in $CD8^+$ T cells following P-YE treatment. Assembled NOX complex releases super oxide (O^{2-}) and unstable O^{2-} promptly converts to hydrogen peroxide (H_2O_2).

Therefore, to confirm ROS level, H_2O_2 was indirectly measured by treating cells with DCFDA, which is oxidized to DCF and emits fluorescence upon reacting with intracellular H_2O_2 (Fig.7A). In the OGD-CM group, ROS levels were about 9-folds higher than in the control group, but decreased by 8-fold after P-YE treatment (Fig.7B). And the expression levels of NADPH oxidase (NOX), which mediates the ROS generation process, were confirmed through WB (Fig.7C). The expression level was decreased by about 1.75-fold in the O+P-YE group compared to the OGD-CM group (Fig.7D).

It can be interpreted that when P-YE is treated, the binding of P-YE to NCF1 prevents NCF1 from joining the NOX complex, which consequently leads to a reduction in ROS production.

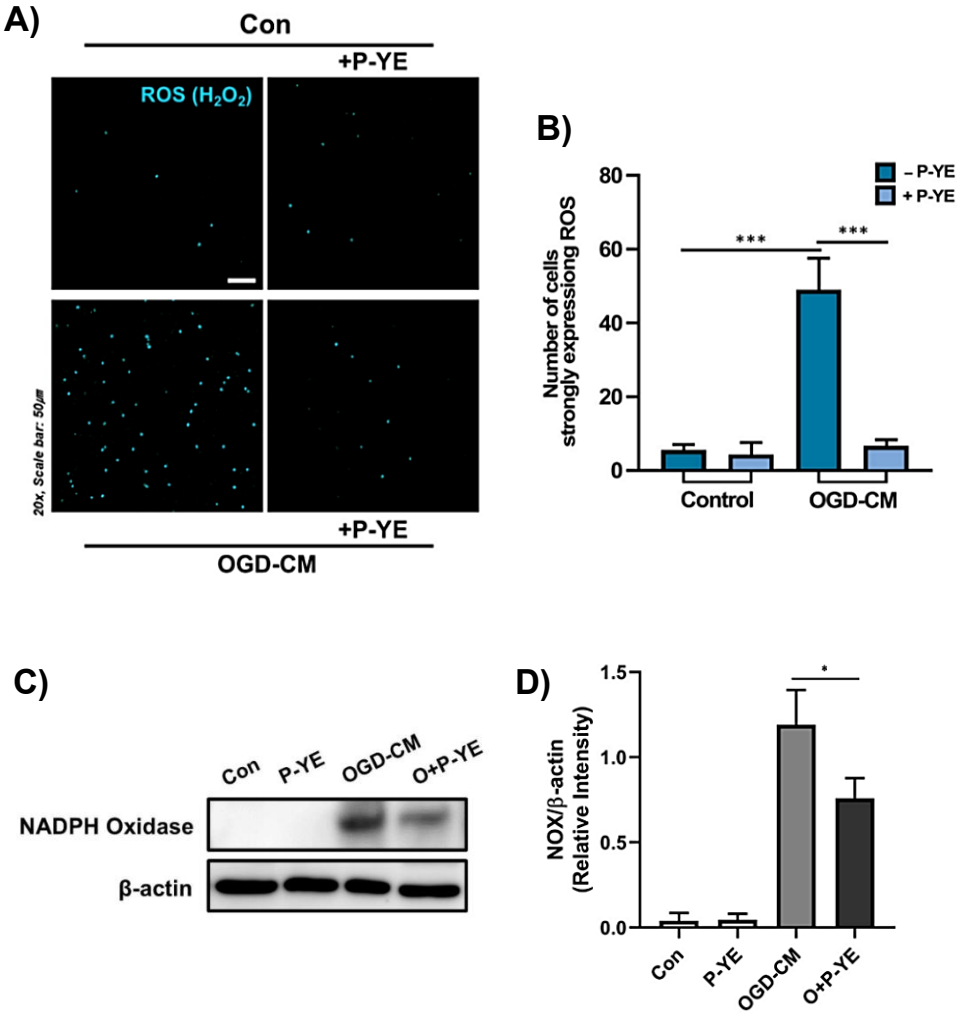

Fig 7. Confirmation of ROS expression level via NOX formation and NADPH oxidase expression. A) ROS levels were confirmed using DCFDA, which can bind to H_2O_2 (Scale bar: 50um). B) ROS was significantly decreased in the O+P-YE group compared to the OGD-CM group. C) WB data show expression level of NADPH Oxidase. D) NOX increased sharply in the OGD-CM group and decreased by approximately 1.75-fold after P-YE treatment. (***P-value<0.001, **P-value<0.01, n=3)

3.8. P-YE reduced pro-inflammatory cytokines in an inflammatory environment

To investigate whether a subset of $CD8^+$ T cells expressing FOXP3 following P-YE treatment exhibits anti-inflammatory properties, $CD8^+$ T cell derived conditioned medium were collected and subjected to a cytokine array analysis (Fig.8A). The results showed that pro-inflammatory cytokines like IFN-Ɣ, TNF-α, MIP-2, CCL5 and bifunctional cytokines IL-1ra, IL-27 and MIP1-α were expressed in OGD-CM group but, theses cytokines were decreased about 1.5~3 folds after P-YE treatment (Fig.8B). And the functions and roles of these cytokines are described in Table 1.

The reduction in pro-inflammatory cytokines following P-YE treatment could be interpreted not only as the anti-inflammatory function of a subset of $CD8^+FOXP3^+$ double-positive T cells expressing FOXP3, but also as a result of a chain-like reduction in inflammatory capacity due to decreased ROS release.

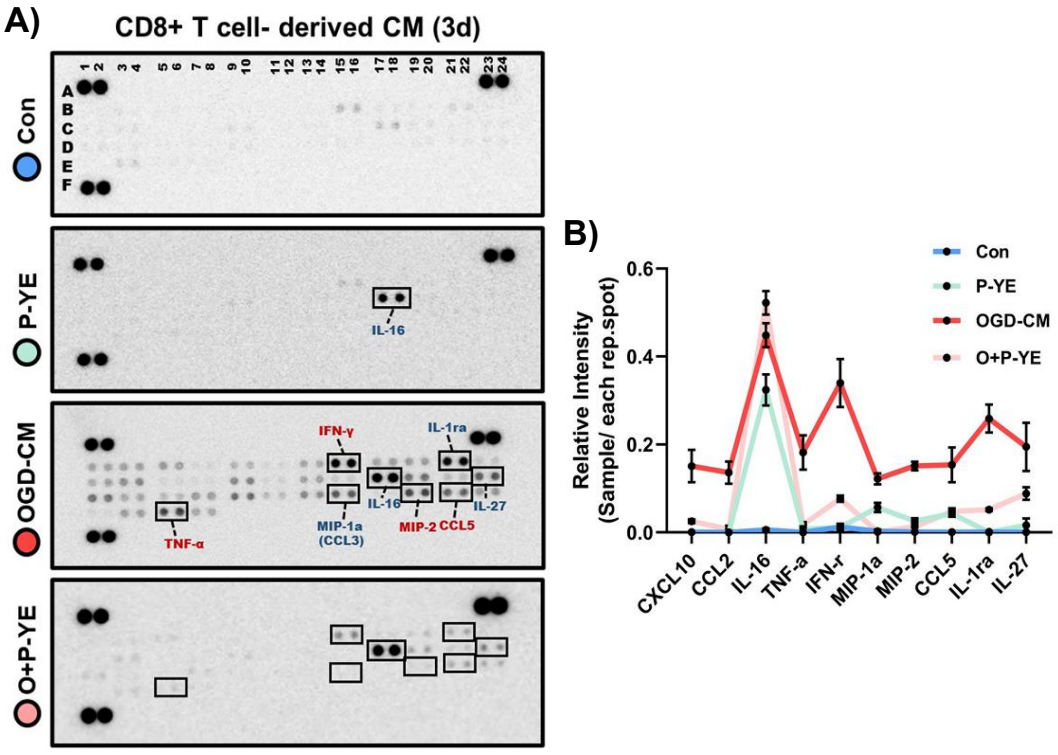

Table1. Types and functions of secreted cytokines in CD8$^+$ T cells

Cytokine	Type	Function
CXCL10	Pro	Interferon gamma-induced protein
CCL2	Pro	Monocyte chemoattractant protein
IL-16	Pro/anti	Chemoattractant for CD4$^+$ cells, as a modulator of T-cell activation
TNF-α	Pro	Acts as an amplifier of inflammation
IFN-Y	Pro	Exerts a negative (proapoptotic) effect on CD8+ T cell responses
MIP-1α	Pro/anti	Recruiting inflammatory cells, wound healing
MIP-2	Pro	Attracts neutrophils to the site of inflammation
CCL5	Pro	Migration of different T cell subsets in immune responses
IL-1rα	Pro/anti	Important in host defense against endotoxin-induced injury
IL-27	Pro/anti	Induces differentiation of the diverse populations of T cells in the immune system

Fig 8. Confirmation of secreted cytokine in CD8$^+$ T cells after P-YE treatment. A) Proteome profiler mouse cytokine array which contained 40 different capture antibodied printed in duplicate. CD8$^+$ T cell derived conditioned medium was used for this experiment. B) The quantification data (Sample/Each reference spot) show that the cytokines expressed in the OGD-CM group were reduced after P-YE treatment. Table) Types and functions of secreted cytokines in CD8$^+$ T cells.

3.9. $CD8^+FOXP3^+$ T cells were partially observed and ROS was decreased following P-YE injection after tMCAO

The degree of tissue damage and mitigation before and after P-YE injection was evaluated in '3.1'. Therefore, specifically, this step aimed to verify the presence of infiltrating $CD8^+$ T cells in the *in vivo* tMCAO group, which showed a 50% tissue damage rate, and to confirm the FOXP3 expressions among the infiltrating $CD8^+$T cells following P-YE injection. In tMCAO group, $CD8^+$ T cells (FITC signal) were infiltrated to the infarct area, but T cells were not observed in the undamaged opposite tissue. After P-YE injection, FOXP3 (Rhod signal) was expressed in a subset of the infiltrating $CD8^+$ T cells (Fig.9B). Quantification data from IHC show that $CD8^+$ T cells decreased by approximately 1.75-fold in the peri-infarct area after P-YE injection following tMCAO, compared to the tMCAO group (Fig.9C). However, $CD8^+FOXP3^+$ T cells were increased by about 9.8-folds after P-YE injection after tMCAO compared to the tMCAO group (Fig.9D). By calculating the ratio of $CD8^+$ cells to $CD8^+FOXP3^+$ cells, it was confirmed that the $CD8^+/CD8^+FOXP3^+$ ratio decreased by approximately 26-fold after P-YE treatment (Fig.9E). In the WB analysis performed to re-quantify the overall expression levels beyond the partial infarct area (Fig. 9F), CD8 showed a relatively minor difference in expression levels of about 1.2-fold between the tM and tM+P groups (Fig.9G), as it reflects the expression of both $CD8^+$ T cells and $CD8^+FOXP3^+$ T cells. However, FOXP3 expression in the tM+P group was approximately 1.8 times higher than that in the tM group (Fig.9F, H). Additionally, ROS levels were analyzed through DHE (1 mg/kg) injection. Among the various types of ROS, O_2^- was detected by its binding to DHE (Fig. 9I). After tMCAO surgery, ROS levels increased about 3-folds compared to the Sham group, but following P-YE injection, they decreased by about 2-folds in peri-infarct area (Fig.9J) and there were no changes in contralateral (Fig.9K).

Based on evidence from *in vitro* experiments, this data suggests that after P-YE injection, some $CD8^+$ T cells migrating to the peri-infarct area express FOXP3. Furthermore, since the changes in ROS levels were observed in the same region as shown in Fig. B, combined with the *in vitro* ROS assay results showing a decrease in ROS levels following P-YE treatment on $CD8^+$ T cells, these changes in ROS levels can be interpreted as being influenced, at least in part, by certain $CD8^+$ T cells and $CD8^+FOXP3^+$ T cells among the various cell types present in the region.

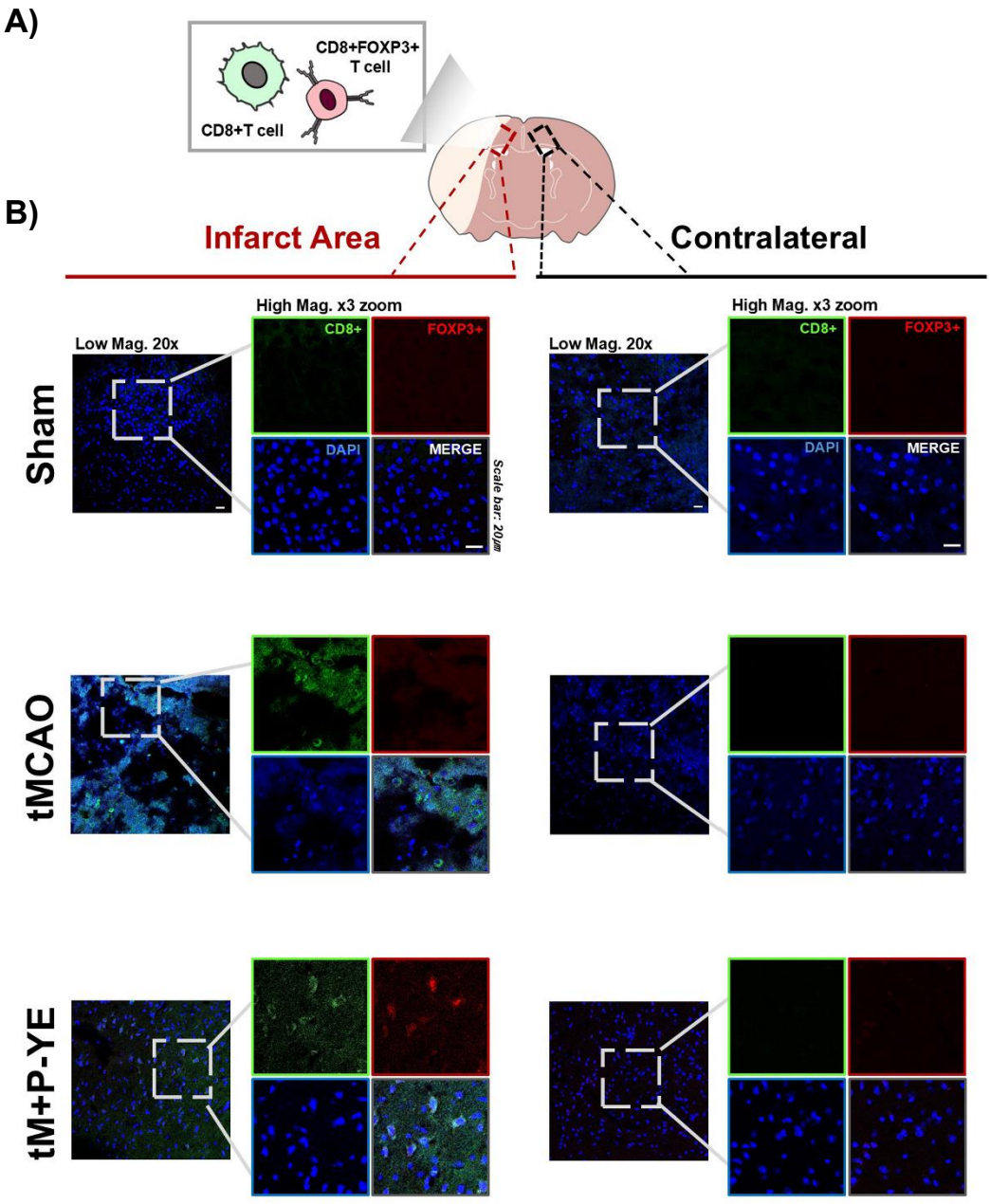

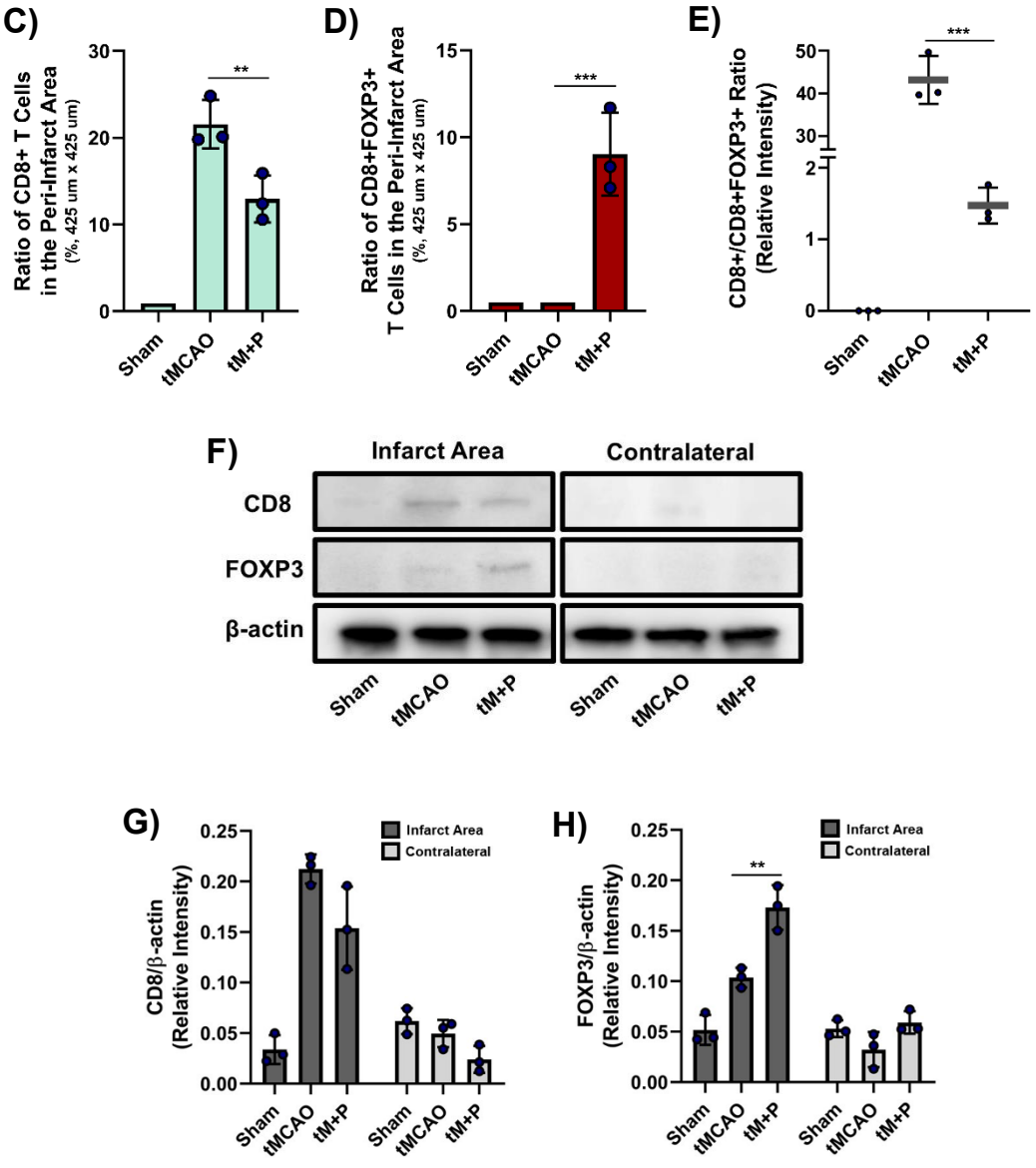

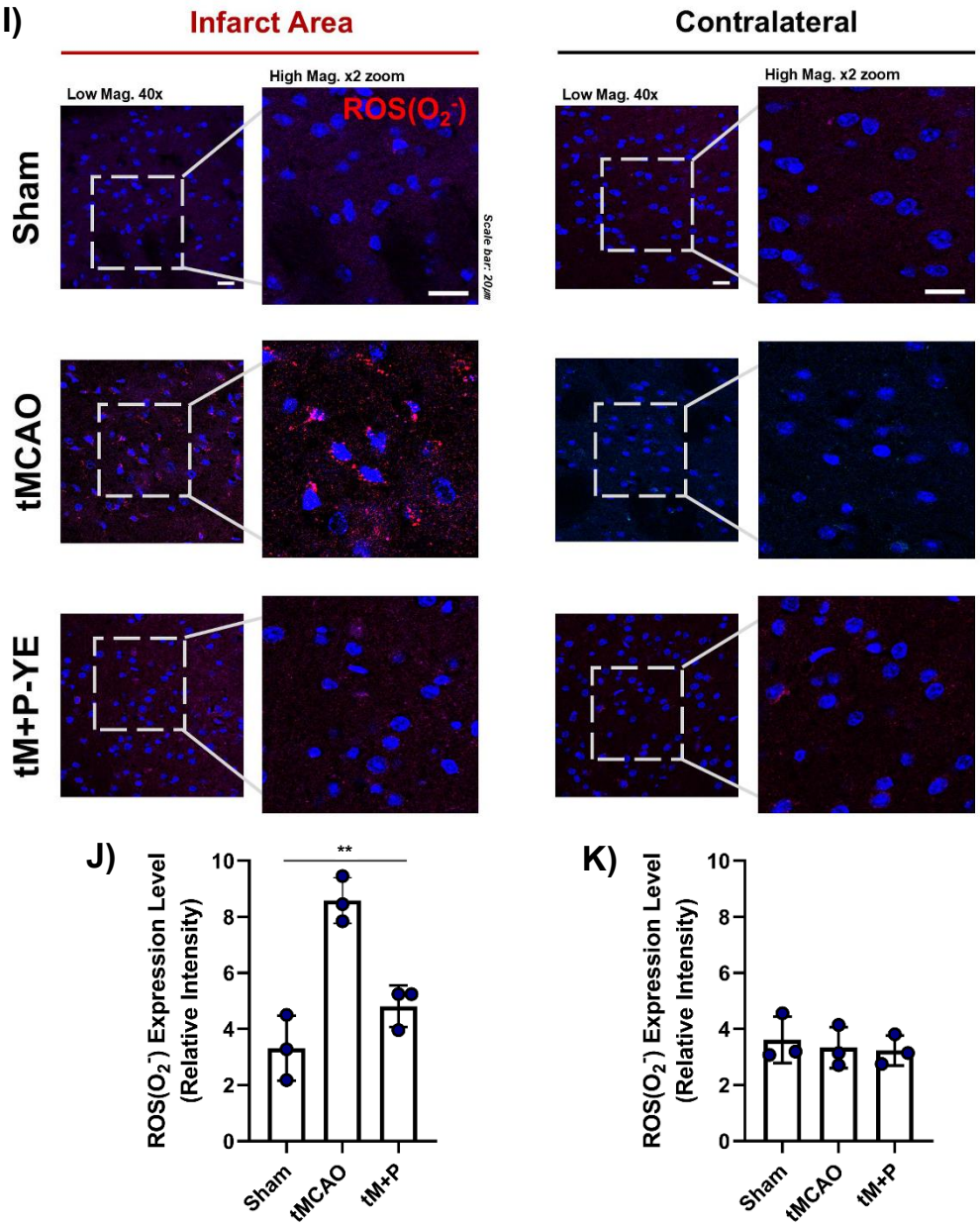

Fig 9. FOXP3 expression in CD8+ T cells recruited *in vivo* and their impact on ROS levels.

A) The presence of $CD8^{+}$T cells that migrated to the infarct area after tMCAO surgery was confirmed. The figure illustrates the location within the whole brain where imaging was performed and indicates that T cells were targeted and captured in that specific region. B) IHC data show the

presence of $CD8^+$T cells that migrated to the area surrounding the infarct, as well as the expression of FOXP3 in $CD8^+$ T cells. (Scale bar: 20um) C, D and E) The quantification data show the ratio of $CD8^+$T cells or $CD8^+FOXP3^+$T cells among total cells (DAPI stained cells) and $CD8^+/FOXP3^+$ ratio in the peri-infarct area. (An 18 mm^2 area near the infarct region around the blood vessels entering the cerebral cortex was imaged, and the number of cells within this area was counted using ImageJ) F, G and H) The WB data show the differences in CD8 and FOXP3 expression among total proteins extracted from the infarct-side hemisphere and the contralateral hemisphere. I) IHC data show the expression level of ROS in the same area where $CD8^+$ T cells were observed in the peri-infarct region. (Scale bar: 20um) J and K) The quantification data show ROS expression levels. (***P-value<0.001, **P-value<0.01, *P-value<0.05, n=3)

3.10. Microglia with a pro-inflammatory phenotype was decreased around the site of injury after P-YE injection

Microglia are brain-resident macrophages that can be affected by other types of infiltrating immune cells and can change their phenotype according to the type of stimuli[29,30]. The immediately preceding results examined $CD8^+$ T cells and $CD8^+FOXP3^+$ T cells before and after P-YE treatment following tMCAO. Therefore, the correlation between changes in the types of infiltrating cells and the pro-inflammatory and anti-inflammatory phenotypic changes of microglia was investigated. CD86 (FITC signal), which represents the pro-inflammatory phenotype of microglia, was clearly observed in the area surrounding the infarct region following tMCAO surgery (Fig.10B). After P-YE treatment, CD86 was decreased by about 2-folds in the same area, compared to tMCAO group but contrary to expectations, the expression of CD206 was not observed (Fig.10C, D and E).

The WB data show that in the tM group, CD86 expression was approximately 1.8-fold higher than in the tM+P group in the infarct hemisphere (Fig.10F, G). CD206 did not show a significant difference in expression levels (Fig.10H)

And also, CD86 was not detected in the sham group and in the contralateral regions of any group, suggesting that its expression was specifically induced by pro-inflammatory stimuli associated with tMCAO surgery. Based on our immediately preceding data, it can be inferred that one of the pro-inflammatory stimuli may have been the infiltrated $CD8^+$ T cells. The key point is the interpretation of the reduction in CD86 following P-YE treatment. Primarily, this could be considered a result of the weakened pro-inflammatory function of the converted $CD8^+FOXP3^+$ cells after P-YE treatment; however, other influences cannot be ruled out.

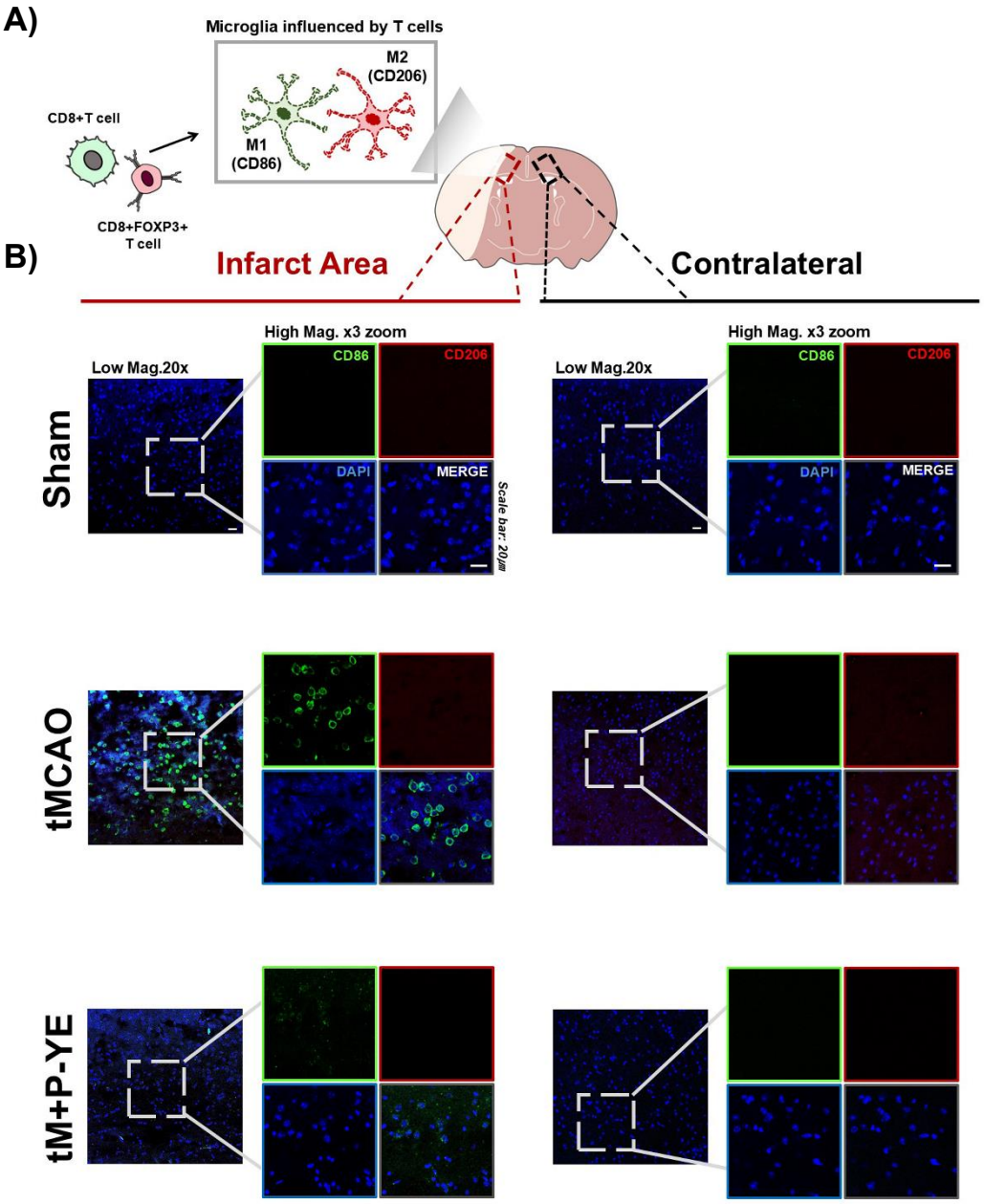

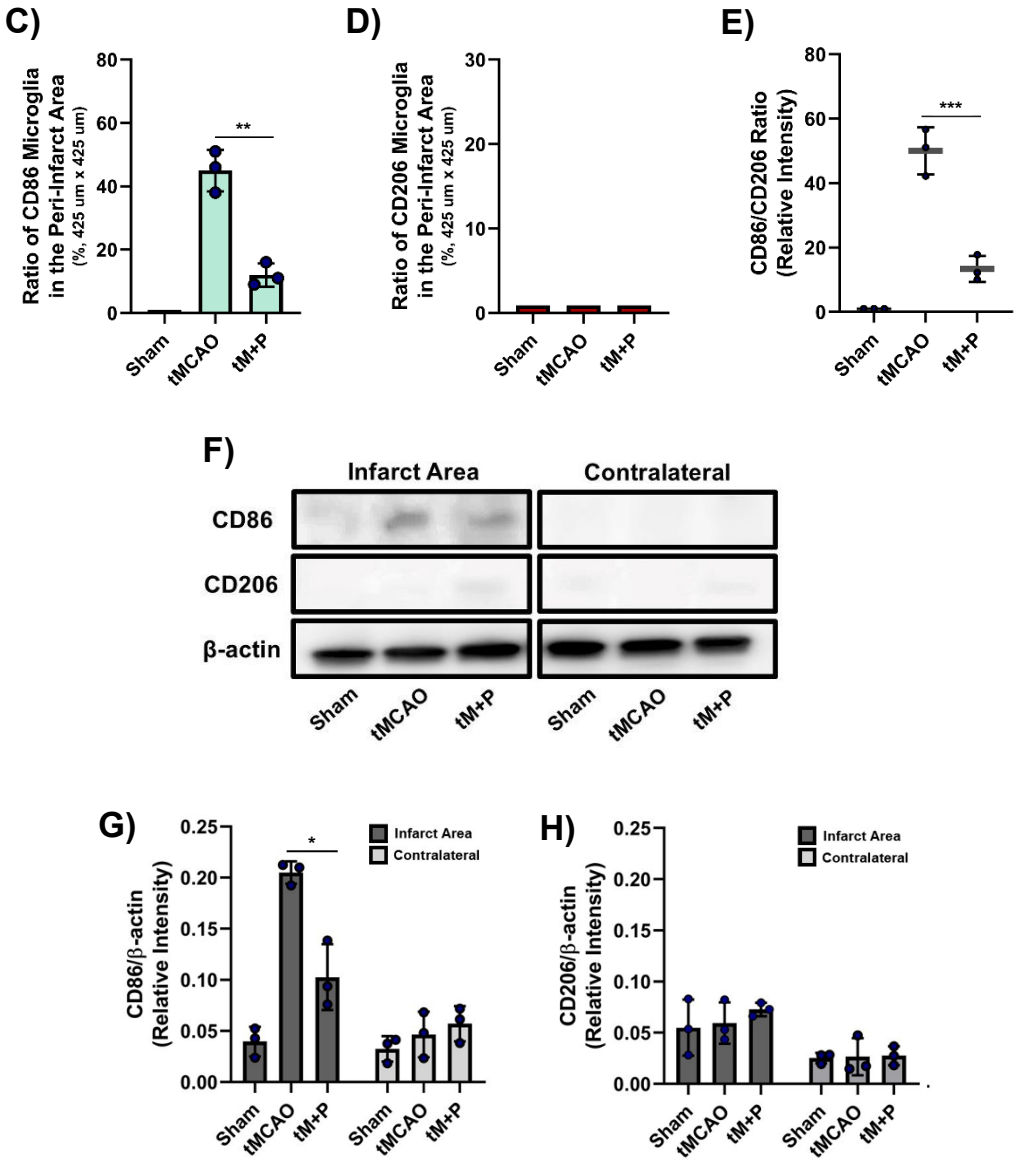

Fig 10. The Pro/anti phenotypes of microglia affected by recruiting T cells were confirmed *in vivo*. A) The figure illustrates the location within the whole brain where imaging was performed and indicates that microglia which was influenced by T cell subsets were targeted and captured in that specific region. B) IHC data show two types of microglia in the area surrounding the infarct: the pro-inflammatory phenotype (CD86; M1) and the anti-inflammatory phenotype (CD206; M2).

(Scale bar: 20um) C, D and E) The quantification data show the ratio of M1 or M2 microglia cells among total cells (DAPI stained cells) and $CD8^+/FOXP3^+$ ratio in the peri-infarct area. (An 18 mm^2 area near the infarct region around the blood vessels entering the cerebral cortex was imaged, and the number of cells within this area was counted using ImageJ) F, G and H) The WB data show the differences in CD86 and CD206 expression among total proteins extracted from the infarct-side hemisphere and the contralateral hemisphere. (***P-value<0.001, **P-value<0.01, *P-value<0.05, n=3)

4. Discussion

The fundamental purpose of this study was to minimize tissue damage and preserve unaffected tissue as much as possible by regulating cytotoxic T cells ($CD8^+$ T cells), which are a major factor exacerbating tissue damage as one of the adaptive immune cells involved in the intricate immune response following brain ischemic injury.

This study began with the identification of T cells infiltrating after ischemic injury as potential targets, and the immune modulator P-YE was chosen to regulate their function. To determine the specific target T cell, a protein micro-array chip experiment was conducted, which revealed that P-YE interacts with NCF1. Based on these results, the focus was narrowed down to suppressing $CD8^+$ T cells. It was found that P-YE binds with NCF1, affecting the existing NCF1-Moesin complex which can be formed during inflammatory responses. This binding inhibited NOX formation and redirected Moesin to other cellular signaling pathways. Consequently, this process inhibited ROS release and induced FOXP3 expression, thereby suppressing the pro-inflammatory functions of cytotoxic T cells and contributing to tissue protection.

As briefly explained in the introduction, during the reperfusion process following ischemic brain injury, the compromised blood-brain barrier (BBB) allows the influx of numerous immune cells besides $CD8^+$T cells[31]. These include cells involved in the innate immune response as well as those responsible for the adaptive immune response, which enter with a slight temporal difference[32,33].

Typically, myeloid cells that initiate the innate immune response are the first to infiltrate the inflamed area, forming the initial line of defense[34]. However, these cells lack diversity in terms of specialized subtypes rather than T cells[35,36], which means targeting them can lead to various side effects. While myeloid cells can release reactive oxygen species (ROS), potentially causing damage to surrounding healthy tissue, they also play a crucial role in clearing dead cells and debris from the damaged tissue and promoting regeneration. Since specific subtypes are not solely responsible for each of these tasks, broad suppression of myeloid cells could delay the clearing process, ultimately hindering tissue regeneration and slowing recovery. Also, in the case of microglia, the primary cells

involved in brain inflammation, they are not cells that infiltrate after reperfusion, but rather brain-resident macrophages. These cells trigger an inflammatory response within minutes of the onset of ischemic injury[37]. As a result, by the time therapeutic interventions become feasible post-reperfusion, microglia have already initiated significant inflammatory activity[38]. Given this early activation, targeting microglia in this study, which aimed to regulate cells that could be modulated during the reperfusion phase, posed challenges. Therefore, microglia, which had already played a key role in the inflammatory response by the time of reperfusion, were not prioritized as a target in this research.

T cells, which mediate a precise adaptive immune response, infiltrate the ischemic tissue after innate immune cells. The timing of their infiltration varies depending on their subtypes, with some T cells entering the damaged area a few hours after reperfusion and others continuing to arrive up to a month post-injury[8]. During ischemic injury, T cells perform distinct functions depending on their subtype, with some types exhibiting cytotoxic activity while others have anti-inflammatory effects[39]. Since each T cell subtype is specialized for a specific immune response, targeting certain T cells to regulate inflammation may effectively suppress unnecessary immune reactions at the injury site, while still maintaining essential defense mechanisms. This strategy has the potential to control inflammation without hindering the overall immune response required for recovery. Therefore, the approach of either converting cytotoxic T cells into anti-inflammatory types or increasing the population of existing anti-inflammatory T cells to minimize the inflammatory response was considered.

During this process, the immune modulator P-YE was identified and highlighted its potential in modulating immune responses through previous studies. In those studies, about P-YE demonstrated anti-inflammatory effect after P-YE injection in organophosphate-induced inflammation model and MCAO models[16,17]. In the areas where the anti-inflammatory effects were observed, the recruitment of Treg cells was consistently confirmed across studies. However, there has been no experimental evidence demonstrating the mechanism by which these anti-inflammatory Treg cells were recruited after P-YE treatment. The reports have been purely phenomenological. Therefore, this study aimed to understand the principle and importance of T cell regulation in the brain disease such as ischemic injury by proposing the precise mechanism by which P-YE regulates T cells to produce its anti-inflammatory effects. For this, it was important to find proteins that could

interact with P-YE, and a protein micro-array chip experiment was conducted.

As shown in the results of Result 2, P-YE strongly bound to five types of proteins based on the A-score, among which the factor directly related to T cell immunity was Neutrophil cytosolic factor 1 (NCF1). As the name suggests, This NCF1 is primarily found in neutrophils and is a component of the NOX complex, which contributes to the release of reactive oxygen species (ROS). However, NCF1 is not limited to neutrophils; it is also commonly found in other cell types that secrete ROS, such as microglia and T cells[40-42]. In these cells, NCF1 moves to the cell membrane in inflammatory environments, where it assembles with the NOX complex. This process involves NCF1 binding with PX domain of Moesin, a cytoskeletal protein[28], which guides NCF1 to the membrane to facilitate its integration into P22, one of the transmembrane components of the NOX complex[43]. This Moesin which carry out NCF1 to the cell membrane is a basically multifunctional protein[26,43,44] that performs its role in a context-dependent manner by joining the more dominant reaction among the reactions in which it can participate depending on the cellular state. For instance, in cases where cytotoxic functions predominate, such as with $CD8^+$ T cells, Moesin integrates into signaling pathways related to inflammation or cell death. Conversely, in cases where immunosuppression predominates, such as in Treg cells, Moesin can contribute to immunoregulatory function by engaging the FOXP3 expression signaling pathway in the presence of factors that phosphorylate Moesin, such as TGF-beta or TNF-alpha[45-47].

According to the protein microarray results, P-YE strongly bound to NCF1, which performs these functions, so it was thought that treating cells with P-YE would inhibit the function of NCF1 and allow Moesin to enter other cell signaling pathways. According to this hypothesis, the target cells needed to have pre-existing pro-inflammatory and cytotoxic functions, and it was considered that P-YE treatment would contribute to tissue protection by weakening these functions.

Among the T cell subsets that release ROS when NCF1 is expressed intracellularly, $CD8^+$ T cells were the most appropriate target cells. This is because, following cerebral ischemic injury, $CD8^+$ T cells infiltrate the infarct area within hours to up to 3 days, at a relatively early time point , establishing the basis for determining the extent of damage through the compromised BBB[8] and, influenced by immune tolerance suppression triggered by the inflammatory environment, subsequently attack not only damaged neurons but also unintended healthy neurons. When their original cytotoxic function is exaggerated, they cause greater damage than any other cells, playing

a key detrimental role as adaptive immune cells that exacerbate tissue damage[15 48-51]. Certainly, while some $CD4^+$ T cells also release ROS and contribute to pro-inflammatory responses, $CD4^+$ T cells primarily participate in immune responses indirectly through cytokine secretion rather than direct cytotoxic mechanisms[52]. Unlike $CD8^+$ T cells, $CD4^+$ T cells can differentiate into anti-inflammatory phenotypes depending on the duration and conditions of the inflammatory response. Thus, to achieve a more precise and definitive effect, $CD8^+$ T cells were selected as the primary target T cell subset.

After $CD8^+$ T cells were identified as the target cells to be regulated, the introduction of P-YE specifically into $CD8^+$ T cells was considered. In an attempt to achieve this, PLGA-based nanoparticles, which are biodegradable and capable of efficiently delivering substances into cells, were tried to conjugate with CD8 antibodies to facilitate the delivery of P-YE. However, due to experimental limitations, this approach could not be fully implemented. Therefore, although it was not specific to $CD8^+$ T cells, in order to enhance the efficiency of P-YE delivery into cells, it was packaged into nanoparticles before conducting the experiment.

To mimic the reperfusion environment encountered by $CD8^+$ T cells infiltrating the infarcted area, microglia were cultured in an OGD chamber for 1 hr, and the cytokines secreted during this process were collected and applied to $CD8^+$ T cells. Microglia, as brain-resident macrophages, initiate a response within minutes after the onset of occlusion, secreting pro-inflammatory cytokines like TNF-α, IRF-Ɣ to trigger an immune reaction in the early phase[53]. Theoretically, $CD8^+$ T cells are known to infiltrate the brain between several hours and up to three days post-reperfusion. Thus, the environment encountered by $CD8^+$ T cells during this period is influenced by the inflammatory cytokines secreted by microglia, which served as the rationale for the experimental conditions set in this study. After treatment with microglia-derived OGD-CM and P-YE in isolated $CD8^+$ T cells, NCF1 bound to P-YE instead of Moesin, and FOXP3 was expressed. Consequently, the release of ROS and pro-inflammatory cytokines was inhibited. However, in these results examining molecular levels, the expression rate of FOXP3 in the flow cytometry data was approximately 15%, which was lower than expected. This issue could potentially be improved if the amount of P-YE entering the cells increases. According to the current results of this study, approximately 50% of P-YE has been internalized into the cells. However, if future advancements resolve the problem of CD8 antibody conjugation on nanoparticles, making it possible to more specifically target $CD8^+$ T cells, it is

expected that a higher expression level will be observed compared to the current results.

Also, based on the results from the ROS assay and the cytokine array, it was confirmed that these molecular-level changes led to actual anti-inflammatory effects. ROS levels were reduced, and there was a decrease in cytotoxic pro-inflammatory cytokines. In the cytokine array, among the various types of cytokines, IL-16, which functions as a chemoattractant for $CD4^+$ T cells, was expressed in all groups except the control. Although this has not yet been clarified, it is speculated that P-YE itself induces the secretion of IL-16 based on this data and previous reports about P-YE. In fact, previous studies on P-YE presented in the introduction have shown that it promotes the recruitment of Treg cells. This suggests the possibility that IL-16 secretion, triggered through an unconfirmed mechanism, might have led to the recruitment of $CD4^+$ T cells, from which differentiated $CD4^+CD25^+$ Treg cells were detected. However, the focus of this study was not on elucidating the correlation between P-YE and IL-16. Instead, it concentrated on targeting $CD8^+$ T cells through the P-YE-NCF1 relationship, as demonstrated by the protein microarray chip results, which were conducted to verify other precise mechanisms. Consequently, this data focused solely on the overall reduction of pro-inflammatory cytokines.
This outcome, which showed a decrease in ROS and pro-inflammatory cytokines, is likely not solely due to the 15% of converted $CD8^+FOXP3^+$ T cells but rather because the converted cells may have suppressed the chain activation of surrounding unconverted $CD8^+$ T cells to some extent. For example, within the same $CD8^+$ T cell population, cells may undergo chain activation influenced by ROS released by one another; however, some converted cells can inhibit this chain overactivation.
In fact, previous studies have shown that converted $CD8^+FOXP3^+$ T cells, which exhibit regulatory and immunosuppressive characteristics similar to Treg cells[54], are known to release anti-inflammatory cytokines or directly suppress the activity of effector T cells through cell-cell contact mechanisms[55,56]. These regulatory functions can also help mitigate the overactivation of surrounding cytotoxic $CD8^+$ T cells, thereby reducing the overall inflammatory response.

In *in vivo* data using the tMCAO mouse model, FOXP3 expression was observed in the recruited $CD8^+$ T cells in the IHC data after P-YE injection. These $CD8^+FOXP3^+$ T cells were also found to reduce ROS level and the number of pro-inflammatory microglia. Since the administered P-YE was not specifically targeted to $CD8^+$ T cells, it is possible that P-YE entered other cells such as microglia or neutrophils, reducing the pro-inflammatory response and infarct area through

unverified mechanisms. However, based on the mechanisms demonstrated *in vitro* data, it is interpreted that the converted $CD8^+FOXP3^+$ T cells may have been one of the causes of the results showing that they reduced the inflammatory response and reduced the area of damaged tissue.

Therefore, this study is significant in that it demonstrates the molecular mechanism by which the cytotoxic function of $CD8^+$ T cells is weakened through the immunomodulator P-YE, and highlights one of the effects on tissue when their anti-inflammatory function is subsequently enhanced. Through the development of $CD8^+$ T cell-specific targeting nanoparticles in further studies, a clearer demonstration of the effects range of P-YE-induced $CD8^+FOXP3^+$ T cells in modulating the neuroinflammatory response following ischemic brain injury could be achieved. If this approach is realized, it could serve as a foundation for developing therapeutic strategies to control the adaptive immune response, which triggers cytotoxic functions after reperfusion.

5. Conclusion

This study showed that regulation of Cytotoxic $CD8^+$ T cells to $CD8^+FOXP3^+$ T cells by P-YE can alleviate neuroinflammation following ischemic stroke.
The key detailed mechanisms of the aforementioned results discovered in this study are as follows:

- P-YE was strongly bound to NCF1 which is a one part of NOX complex secreting ROS in neuroinflammation environment.

- After P-YE treatment in an inflammation environment, the pre-existing NCF1-Moesin binding complex was decreased, and free phospho-Moesin induced FOXP3 expression.

- These molecular changes reduced ROS release and decreased the secretion of pro-inflammatory cytokines.

- Following P-YE injection after tMCAO surgery *in vivo*, CD8+ T cells infiltrating the infarct area were confirmed to express FOXP3. These cells reduced ROS levels and decreased the number of pro-inflammatory (M1) microglia, thereby mitigating tissue damage. Consequently, this led to improvements in behavioral deficits caused by neuronal damage.

In summary, in a neuroinflammatory environment, $CD8^+$ T cells are converted into anti-inflammatory $CD8^+FOXP3^+$ T cells by P-YE through the modulation of NCF1-Moesin function, which effectively reduces the extent of tissue damage caused by ischemic stroke.

References

1 Joy, M. T. & Carmichael, S. T. Encouraging an excitable brain state: mechanisms of brain repair in stroke. *Nat Rev Neurosci* 22, 38-53, (2021).

2 Kim, J. Y., Park, J., Chang, J. Y., Kim, S. H. & Lee, J. E. Inflammation after Ischemic Stroke: The Role of Leukocytes and Glial Cells. *Exp Neurobiol* 25, 241-251, (2016).

3 Zivancevic, K., Lovic, D., Andjus, P. R. & Radenovic, L. in *Cerebral Ischemia* (ed R. Pluta) (2021).

4 Chen, R., Zhang, X., Gu, L., Zhu, H., Zhong, Y., Ye, Y. et al. New Insight Into Neutrophils: A Potential Therapeutic Target for Cerebral Ischemia. *Front Immunol* 12, 692061, (2021).

5 Liu, P. Y., Li, H. Q., Dong, M. Q., Gu, X. Y., Xu, S. Y., Xia, S. N. et al. Infiltrating myeloid cell-derived properdin markedly promotes microglia-mediated neuroinflammation after ischemic stroke. *J Neuroinflammation* 20, 260, (2023).

6 Jayaraj, R. L., Azimullah, S., Beiram, R., Jalal, F. Y. & Rosenberg, G. A. Neuroinflammation: friend and foe for ischemic stroke. *J Neuroinflammation* 16, 142, (2019).

7 Zhang, D., Ren, J., Luo, Y., He, Q., Zhao, R., Chang, J. et al. T Cell Response in Ischemic Stroke: From Mechanisms to Translational Insights. *Front Immunol* 12, 707972, (2021).

8 Wang, Y. R., Cui, W. Q., Wu, H. Y., Xu, X. D. & Xu, X. Q. The role of T cells in acute ischemic stroke. *Brain Res Bull* 196, 20-33, (2023).

9 Gong, Z., Guo, J., Liu, B., Guo, Y., Cheng, C., Jiang, Y. et al. Mechanisms of immune response and cell death in ischemic stroke and their regulation by natural compounds. *Front Immunol* 14, 1287857, (2023).

10 DeLong, J. H., Ohashi, S. N., O'Connor, K. C. & Sansing, L. H. Inflammatory Responses After Ischemic Stroke. *Semin Immunopathol* 44, 625-648, (2022).

11 Jian, Z., Liu, R., Zhu, X., Smerin, D., Zhong, Y., Gu, L. et al. The Involvement and Therapy Target of Immune Cells After Ischemic Stroke. *Front Immunol* 10, 2167, (2019).

12 Lei, T. Y., Ye, Y. Z., Zhu, X. Q., Smerin, D., Gu, L. J., Xiong, X. X. et al. The immune response of T cells and therapeutic targets related to regulating the levels of T helper cells after ischaemic stroke. *J Neuroinflammation* 18, 25, (2021).

13 Barnaba, V. T Cell Memory in Infection, Cancer, and Autoimmunity. *Front Immunol* 12, 811968, (2021).

14 Yu, Y., Ma, X., Gong, R., Zhu, J., Wei, L. & Yao, J. Recent advances in CD8(+) regulatory T cell research. *Oncol Lett* 15, 8187-8194, (2018).

15 Zhang, Z., Duan, Z. & Cui, Y. CD8(+) T cells in brain injury and neurodegeneration. *Front Cell Neurosci* 17, 1281763, (2023).

16 Finkelstein, A., Kunis, G., Berkutzki, T., Ronen, A., Krivoy, A., Yoles, E. et al. Immunomodulation by poly-YE reduces organophosphate-induced brain damage. *Brain Behav Immun* 26, 159-169, (2012).

17 Ziv, Y., Finkelstein, A., Geffen, Y., Kipnis, J., Smirnov, I., Shpilman, S. et al. A novel immune-based therapy for stroke induces neuroprotection and supports neurogenesis. *Stroke* 38, 774-782, (2007).

18 Ruan, J. & Yao, Y. Behavioral tests in rodent models of stroke. *Brain Hemorrhages* 1, 171-184, (2020).

19 Shimazu, T., Hirschey, M. D., Newman, J., He, W., Shirakawa, K., Le Moan, N. et al. Suppression of oxidative stress by beta-hydroxybutyrate, an endogenous histone deacetylase inhibitor. *Science* 339, 211-214, (2013).

20 Liu, Z., Lanford, R., Mueller, S., Gerhard, G. S., Luscieti, S., Sanchez, M. et al. Siderophore-mediated iron trafficking in humans is regulated by iron. *J Mol Med (Berl)* 90, 1209-1221, (2012).

21 Jackson, S. H., Devadas, S., Kwon, J., Pinto, L. A. & Williams, M. S. T cells express a phagocyte-type NADPH oxidase that is activated after T cell receptor stimulation. *Nat Immunol* 5, 818-827, (2004).

22 Low, Y. H., Asi, Y., Foti, S. C. & Lashley, T. Heterogeneous Nuclear Ribonucleoproteins: Implications in Neurological Diseases. *Mol Neurobiol* 58, 631-646, (2021).

23 Muzio, L., Viotti, A. & Martino, G. Microglia in Neuroinflammation and Neurodegeneration: From Understanding to Therapy. *Front Neurosci* 15, 742065, (2021).

24 You, K., Gu, H., Yuan, Z. & Xu, X. Tumor Necrosis Factor Alpha Signaling and Organogenesis. *Front Cell Dev Biol* 9, 727075, (2021).

25 Koss, M., Pfeiffer, G. R., 2nd, Wang, Y., Thomas, S. T., Yerukhimovich, M., Gaarde, W. A. et al. Ezrin/radixin/moesin proteins are phosphorylated by TNF-alpha and modulate permeability increases in human pulmonary microvascular endothelial cells. *J Immunol* 176, 1218-1227, (2006).

26 Ansa-Addo, E. A., Zhang, Y., Yang, Y., Hussey, G. S., Howley, B. V., Salem, M. et al. Membrane-organizing protein moesin controls Treg differentiation and antitumor immunity via TGF-beta signaling. *J Clin Invest* 127, 1321-1337, (2017).

27 Rasmussen, I., Pedersen, L. H., Byg, L., Suzuki, K., Sumimoto, H. & Vilhardt, F. Effects of F/G-actin ratio and actin turn-over rate on NADPH oxidase activity in microglia. *BMC Immunol* 11, 44, (2010).

28 Michie, K. A., Goodchild, S. C. & Curmi, P. M. G. in *Encyclopedia of Signaling Molecules* (ed Sangdun Choi) 1-7 (Springer New York, 2016).

29 Shu, L., Xu, H., Ji, J., Xu, Y., Dong, Z., Wu, Y. et al. Long-Term Accumulation of T Cytotoxic 1, T Cytotoxic 17, and T Cytotoxic 17/1 Cells in the Brain Contributes to Microglia-Mediated Chronic Neuroinflammation After Ischemic Stroke. *Neuromolecular Med* 26, 17, (2024).

30 Benakis, C., Simats, A., Tritschler, S., Heindl, S., Besson-Girard, S., Llovera, G. et al. T cells modulate the microglial response to brain ischemia. *Elife* 11, (2022).

31 Guo, X., Liu, R., Jia, M., Wang, Q. & Wu, J. Ischemia Reperfusion Injury Induced Blood Brain Barrier Dysfunction and the Involved Molecular Mechanism. *Neurochem Res* 48, 2320-2334, (2023).

32 Beuker, C., Strecker, J. K., Rawal, R., Schmidt-Pogoda, A., Ruck, T., Wiendl, H. et al. Immune Cell Infiltration into the Brain After Ischemic Stroke in Humans Compared to Mice and Rats: a Systematic Review and Meta-Analysis. *Transl Stroke Res* 12, 976-990, (2021).

33 Xie, L., He, M., Ying, C. & Chu, H. Mechanisms of inflammation after ischemic stroke in brain-peripheral crosstalk. *Front Mol Neurosci* 17, 1400808, (2024).

34 Mohamud Yusuf, A., Hagemann, N., Ludewig, P., Gunzer, M. & Hermann, D. M. Roles of Polymorphonuclear Neutrophils in Ischemic Brain Injury and Post-Ischemic Brain Remodeling. *Front Immunol* 12, 825572, (2021).

35 Carnevale, S., Di Ceglie, I., Grieco, G., Rigatelli, A., Bonavita, E. & Jaillon, S. Neutrophil diversity in inflammation and cancer. *Front Immunol* 14, 1180810, (2023).

36 Ganesh, K. & Joshi, M. B. Neutrophil sub-types in maintaining immune homeostasis during steady state, infections and sterile inflammation. *Inflamm Res* 72, 1175-1192, (2023).

37 Kang, C., Sang, Q., Liu, D., Wang, L., Li, J. & Liu, X. Polyphyllin I alleviates neuroinflammation after cerebral ischemia-reperfusion injury via facilitating autophagy-

mediated M2 microglial polarization. *Mol Med* 30, 59, (2024).

38 Zeng, J., Bao, T., Yang, K., Zhu, X., Wang, S., Xiang, W. et al. The mechanism of microglia-mediated immune inflammation in ischemic stroke and the role of natural botanical components in regulating microglia: A review. *Front Immunol* 13, 1047550, (2022).

39 Sun, L., Su, Y., Jiao, A., Wang, X. & Zhang, B. T cells in health and disease. *Signal Transduct Target Ther* 8, 235, (2023).

40 Ding, X., Zhang, M., Gu, R., Xu, G. & Wu, H. Activated microglia induce the production of reactive oxygen species and promote apoptosis of co-cultured retinal microvascular pericytes. *Graefes Arch Clin Exp Ophthalmol* 255, 777-788, (2017).

41 Belikov, A. V., Schraven, B. & Simeoni, L. T cells and reactive oxygen species. *J Biomed Sci* 22, 85, (2015).

42 Efimova, O., Szankasi, P. & Kelley, T. W. Ncf1 (p47phox) is essential for direct regulatory T cell mediated suppression of CD4+ effector T cells. *PLoS One* 6, e16013, (2011).

43 Wientjes, F. B., Reeves, E. P., Soskic, V., Furthmayr, H. & Segal, A. W. The NADPH oxidase components p47(phox) and p40(phox) bind to moesin through their PX domain. *Biochem Biophys Res Commun* 289, 382-388, (2001).

44 Freymuth, P. S. & Fitzsimons, H. L. The ERM protein Moesin is essential for neuronal morphogenesis and long-term memory in Drosophila. *Mol Brain* 10, 41, (2017).

45 Gu, J., Zhou, J., Chen, Q., Xu, X., Gao, J., Li, X. et al. Tumor metabolite lactate promotes tumorigenesis by modulating MOESIN lactylation and enhancing TGF-beta signaling in regulatory T cells. *Cell Rep* 39, 110986, (2022).

46 Satooka, H., Nagakubo, D., Sato, T. & Hirata, T. The ERM Protein Moesin Regulates CD8(+) Regulatory T Cell Homeostasis and Self-Tolerance. *J Immunol* 199, 3418-3426, (2017).

47 Takahashi, E., Nagano, O., Ishimoto, T., Yae, T., Suzuki, Y., Shinoda, T. et al. Tumor necrosis factor-alpha regulates transforming growth factor-beta-dependent epithelial-mesenchymal transition by promoting hyaluronan-CD44-moesin interaction. *J Biol Chem* 285, 4060-4073, (2010).

48 Bitar, L., Puig, B., Oertner, T. G., Denes, A. & Magnus, T. Changes in Neuroimmunological Synapses During Cerebral Ischemia. *Transl Stroke Res*, (2024).

49 Stanzione, R., Forte, M., Cotugno, M., Bianchi, F., Marchitti, S. & Rubattu, S. Role of DAMPs and of Leukocytes Infiltration in Ischemic Stroke: Insights from Animal Models and Translation to the Human Disease. *Cell Mol Neurobiol* 42, 545-556, (2022).

50 Zhao, J., Roberts, A., Wang, Z., Savage, J. & Ji, R. R. Emerging Role of PD-1 in the Central Nervous System and Brain Diseases. *Neurosci Bull* 37, 1188-1202, (2021).

51 Salminen, A. The role of the immunosuppressive PD-1/PD-L1 checkpoint pathway in the aging process and age-related diseases. *J Mol Med (Berl)* 102, 733-750, (2024).

52 Gu, L., Jian, Z., Stary, C. & Xiong, X. T Cells and Cerebral Ischemic Stroke. *Neurochem Res* 40, 1786-1791, (2015).

53 Zhang, Y., Lian, L., Fu, R., Liu, J., Shan, X., Jin, Y. et al. Microglia: The Hub of Intercellular Communication in Ischemic Stroke. *Front Cell Neurosci* 16, 889442, (2022).

54 Giri, S., Meitei, H. T., Sonar, S. A., Shaligram, S. & Lal, G. In vitro-induced Foxp3(+) CD8(+) regulatory T cells suppress allergic IgE response in the gut. *J Leukoc Biol* 112, 1497-1507, (2022).

55 Buchwald, Z. S., Kiesel, J. R., DiPaolo, R., Pagadala, M. S. & Aurora, R. Osteoclast activated FoxP3+ CD8+ T-cells suppress bone resorption in vitro. *PLoS One* 7, e38199, (2012).

56 Sanders, J. M., Jeyamogan, S., Mathew, J. M. & Leventhal, J. R. Foxp3+ regulatory T cell

therapy for tolerance in autoimmunity and solid organ transplantation. *Front Immunol* 13, 1055466, (2022).

Appendices

A-

A-score: Assignment Score**, ANOVA:** Analysis of Variance

B-

BBB: Blood Brain Barrier, **BDH2**: 3-Hydroxybutyrate Dehydrogenase 2, **BSA**: Bovine Serum Albumin, **$BSS_{0.0}$**: Balanced Salt Solution$_{0.0}$

C-

CCA: Common Carotid Artery, **CD**: Cluster of Differentiation**, CCL**: C-C Motif Chemokine Ligand, **Con**: Control, **CM**: Conditioned Medium, **Cyto T**: Cytotoxic T cell, **CXCL**: C-X-C motif chemokine ligand

D-

DAPI: 4′,6-diamidino-2-phenylindole, **DCFDA**: 2′,7′-Dichlorofluorescin Diacetate, **DHE**: Dihydroethidium

E-

ECA: External Carotid Artery

F-

FACS: Fluorescence-Activated Cell Sorting, **FITC**: Fluorescein Isothiocyanate, **FOXP3**: Forkhead box P3

G-

Glu: Glutamic acid

H-

HRP: Horseradish Peroxidase, **hnRNP A/B**: heterogeneous nuclear Ribonucleoprotein A/B,

HNRNPD: Heterogeneous Nuclear Ribonucleoprotein D

I-

ICA: Internal Carotid Artery, **ICC**: Immunocytochemistry, **Ig**: Immunoglobulin, **IL-**: Interleukin-, **IFN-Y**: Interferon Gamma, **IHC**: Immunohistochemistry

M-

MCAO: Middle cerebral artery occlusion, **MIP**: Macrophage Inflammatory Protein, **MSN**: Moesin

N-

NADPH: Nicotinamide Adenine Dinucleotide Phosphate, **NCF1**: Neutrophil Cytosolic Factor1, **NCL**: Nucleolin, **Neg**: Negative, **NOX**: NADPH Oxidase, **NP**: Nanoparticle

O-

OD: Oxidase**, OGD**: Oxygen Glucose Deprivation, **O/N**: Overnight, **O+P-YE**: OGD-CM+P-YE

P-

PBS: Phosphate buffer saline**, PI**: Propidium Iodide, **PLGA**: Poly-Lactic Acid-Glycolic Acid, **Pos**: Positive, **PRB3**: Prolin Rich Proetin BstNI Subfamliy 3, **PRH1:** Proline-Rich Protein HaeIII subfamily 1, **P-value**: Probability-value, **PVDF**: Polyvinylidene difluoride, **P-YE**: Poly-Glu/Tyr

R-

RALYL: RALY RNA Binding Protein Like**, ROS**: Reactive Oxygen Species, **RT**: Room temperature

S-

SDF1: Stromal Cell-Derived Factor 1, **SDS-PAGE:** Sodium Dodecyl Sulfate - Polyacrylamide Gel Electrophoresis, **Sup**: Supernatant

T-

TCA: Tricarboxylic Acid**, tMCAO**: transient Middle Cerebral Artery Occlusion, **tM+P**: tMCAO+P-YE, **TNF-α**: Tumor Necrosis Factor-alpha, **Treg cell**: regulatory T cell, **TTC**: 2,3,5-

Triphenyltetrazolium Chloride, Tyr: Tyrosine

W-

WB: Western Blot

Abstract in Korean

뇌 허혈성 손상 후 T세포 조절을 통한 신경 염증 조절 기전

본 연구는 T 세포 조절을 통해 허혈성 뇌졸중 후 발생하는 신경 염증 반응을 완화할 수 있는 기전에 관한 내용을 담고 있다. 허혈성 뇌졸중이 발생하면 신경염증 반응, 세포 대체, 기능 회복의 세 가지 주요 단계를 거치며 증상이 진행되는데 첫 번째 신경염증 반응 가속화 단계에서 비 가역적인 신경 손상이 발생하기 때문에 이 초기 단계를 조절하는 것이 중요하다. 초기 신경염증 반응 단계에서는 다양한 세포들이 손상된 혈액-뇌 장벽을 통해 침투하며, 그 중에서도 세포독성 T 세포(Cyto T)는 경색 부위에서 신경염증을 증폭시키며 신경세포의 직접적인 사멸을 유도한다.

T 세포 조절을 통한 염증반응 완화에 관한 보고를 담고 있는 선행연구들에 의하면 다른 효과기 T 세포 대비, 조절 T 세포(Treg) 비율을 증가시키면 염증 상태를 완화할 수 있음을 보여주었다. 특히, 면역 조절제로 알려진 Poly-Glu/Tyr(P-YE)를 마우스에 주사하면 염증 유발 부위 주변에 Treg 세포의 양이 증가하고 이로 인해 신경 손상으로 인한 행동기능 저하가 개선되었다는 보고들이 있지만, 그 기전은 아직 규명되지 않았다. 따라서 본 연구에서는 P-YE 와 상호작용하는 인자를 선별하고 이러한 상호작용이 어떻게 T 세포를 조절하여 신경염증 반응을 완화하는지 그 기전을 규명하고자 하였다.

먼저 P-YE와 상호작용하는 인자를 찾아내기 위해 단백질 마이크로 어레이 실험을 실시하였으며, P-YE는 21,000개의 종류의 단백질을 포함한 어레이 칩에 반응되었다. *in vitro* 실험에서 8주령 C57BL/6 수컷 마우스의 비장으로부터 Cyto T 세포($CD8^+$ T)를 분리하였으며, 재관류 후 조직내 유입 시 신경염증인자가 방출된 환경에 노출되는 상황을 모방하기 위해 산소-포도당 결핍 조건 미세아교세포 배지(OGD 조건 배지,

OGD-CM)에서 P-YE가 탑재된 나노입자 (Np P-YE)와 함께 24시간동안 배양되었다. 또한, tMCAO 수술을 진행한 생체 실험에서 P-YE는 CCA를 통해 주사 되어 MCA부근까지 유입될 수 있도록 하였다.

그 결과, P-YE는 tMCAO 수술 후 경색 부피를 감소시키고 행동 기능을 개선하였으며, 이러한 현상학적 결과의 원인이 되는 기전을 밝히기 위한 단백질 마이크로어레이 실험에서, P-YE는 ROS를 분비하는 NOX 복합체의 일부인 호중구 세포질 인자 (NCF1)에 강하게 결합하는 것을 확인하였다. 이 NCF1은 염증 반응에서 활성화되어 Moesin에 결합하여 막으로 이동하고 NOX 복합체를 형성하는 것으로 알려져 있으며 이 결과를 바탕으로 해당 기능을 가지고 있는 $CD8^+$세포가 타깃세포로 설정되었다. Co-IP 실험에서는 $CD8^+$T세포에서 P-YE와 NCF1의 결합으로 인해 기존에 결합하고 있던 NCF1-Moesin의 복합체의 감소가 확인되었다. NCF1과 결합하지 않은 Moesin은 FOXP3 발현을 위한 신호전달 경로에 합류될 수 있다는 선행연구를 근거로 진행한 실험에서, O+P-YE 그룹에서 $CD8^+$ T 세포에서 $FOXP3^+$가 발현되는 것을 확인하였으며 이 그룹에서 ROS 및 전 염증성 사이토카인 수치가 현저히 감소하는 것을 확인하였다. P-YE가 주입된 tMCAO 모델링 마우스에서는 경색 부위 주변에서 실제로 $CD8^+FOXP3^+$ T 세포가 이동된 것이 관찰되었으며, 같은 영역에서 ROS 발현양와 전 염증성 표현형인 M1 타입의 미세아교세포의 수가 감소하였다.

결론적으로 분자적 관점에서, P-YE와 결합한 NCF1은 NOX 복합체를 형성하지 못하였고 NCF1로부터 분리된 Moesin은 FOXP3 발현을 유도할 수 있었다.
따라서, 이 연구를 통해 P-YE가 신경염증 조건에서 NCF1에 결합하여 NCF1-Moesin 신호경로에 영향을 미쳐 일부 $CD8^+$ T 세포를 $CD8^+FOXP3^+$ 세포로 전환시킴을 알 수 있었고, 이러한 기전을 통해 결과적으로 ROS 생성과 전 염증성 사이토카인 발현이 억제되어 사멸된 신경세포의 양을 감소시키심으로써 신경학적 손상으로 인한 행동기능 약화를 개선하는 하나의 역할을 수행할 수 있다는 결론을 도출하였다.

핵심되는 말 : 허혈성 뇌졸증, 신경염증반응, 세포독성 T세포, 미세아교세포, P-YE